Dear Editor, dear Dr. Ghislain Picard,

Thanks for the valuable comments, which help to improve the quality of the paper. The detailed replies are addressed below point by point in blue. In short:

(1) More validation is included

	Current version	**Revised version**
Number of site(s)	1	7
Total observation length	1 month	~10 years

(2) The discussion with respect to snow particle shape, especially under different classification systems in different scientific communities.

To retrieve snow properties from satellite observations, what we need is the local optical properties for an "effective particle shape" to perform the radiative transfer calculation, we will emphasize that we should not over-interpret the effective particle shape we retrieved in the revised version. As highlighted in Picard et al (2009), "information is urgently needed to know which model shape best approximates the different type of fresh snow", to address "the uncertainty of SSA retrieval based on the SSA-albedo relationships when grain shape is unknown". We believe our work, as a first step/attempt, provides some new/useful way/information for this issue. And of course, we will introduce a more sophisticated way in our future work, for example, to mix different shapes.

Picard, G., Arnaud, L., Domine, F. and Fily, M., Determining snow specific surface area from near-infrared reflectance measurements: numerical study of the influence of grain shape, Cold regions and science and technology, 56, 10-17,2009

Best regards,

Linlu Mei on behalf of all co-authors

Review "The retrieval of snow properties from SLSTR/Sentinel-3 -part 2: results and validation" by Mei and colleagues. The paper aims at validating an algorithm to retrieve snow grain size and shape, and snow specific surface area from the space-borne SLSTR sensor. The algorithm was described in another paper in review (companion part 1), the present manuscript is dedicated to the validation. The overall goal of these two parts is of interest for the cryosphere community, in particular because SLSTR is on the Sentinel 3 series of satellite which will be able for decades. The paper is original and clear. Nevertheless, my recommendation is to postpone the acceptance of this paper for three main reasons:

Response: Thanks for the very valuable comments from Dr. Ghislain Picard, after detailed discussion with him by emails, we hope we have a good understanding of all comments here. The key issue, as raised by Dr. Ghislain Picard, is about more validation. This is also raised by the second reviewer of part 2. Although, as mentioned by the reviewer, “I understand that it is hard to obtain enough data for remote sensing validation”, we have started to collect more validation data since we saw the comments on 10 Nov. 2020.

The reason why only SnowEx17 was considered for the validation in the current form, is that, to our best knowledge, this is possible the only campaign providing all three satellite retrieved parameters (SGS, SPS and SSA). Now, the new understanding is that we can use any campaign data, even when only one satellite retrieved parameter is provided in the campaign. Thus, the following campaign data have been collected for an enhanced validation, in short, the validation is largely extended from one single month from the SnowEx17 campaign to a couple of years worldwide (see Fig 1). We believe, that the extended validation will provide a comprehensive understating of the performance of XBAER algorithm.

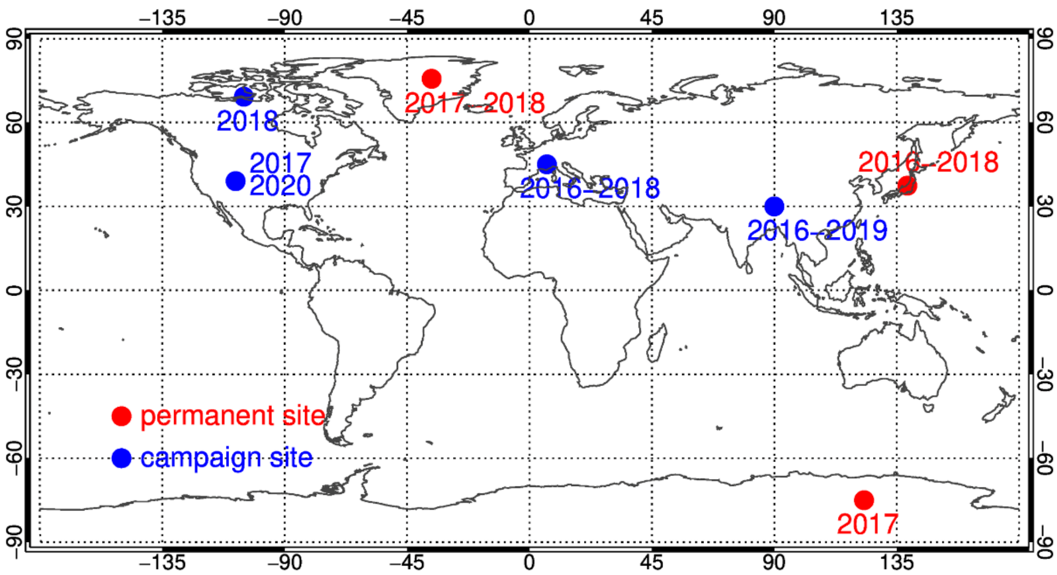

Fig. 1 Geographic distribution of the validation sites. The colors represent the type of each site while the observation period used in this manuscript is indicated near each site.

Please be noted that the above campaign data, covering all typical snow-covered geographic regions, will also provide deeper understanding of potential atmosphere/surface effects. For instance, if we make a cross-validation between the Japanese site and Dome C site, we may have a much better understanding of the impact of aerosol contamination, while the comparison between French Alps and North America may provide more information of the impact of surface elevation.

The validation is based on a too limited set of in-situ data, part of it is discarded because of cloud contamination (SnowEX17). The text truly dedicated to the algorithm performance evaluation is also relatively short and seems unfinished, most of text is about the difficulty to perform the validation, which in the end does not contribute to give confidence in the retrieval algorithm. The conclusion about the algorithm performance therefore lacks of support. There are also several technical issues (see below in the detail comments) in particular one on the RMSE definition. The lack of datasets is a common problem, but not to the extent depicted by the authors. The main example is for the snow grain size. The manuscript cites Kokhanovsky et al. 2019 which pursues a very similar objective as the present manuscript but uses OLCI, (on Sentinel 3 as well as SLSTR) to estimate grain size and SSA (not the grain shape). For the validation these authors used an extensive dataset with 100s of SSA field measurements in Greenland and in Antarctica. These data can be either retrieved from the graphs or in principle obtained from the authors, and should be used here to complete the validation (or even replace the 3 SnowEx measurements). Moreover, the performance between the SLSTR and OLCI algorithms could be analyzed at these in-situ points. At last, the authors "emphasize that the results presented in this section is considered as preliminary" (L373). They indeed propose to include Mosaic data in their analysis in the future. My concern is whether it is worthwhile for the community to publish "preliminary results" in two papers. My suggestion is indeed to wait for complete results and include Mosaic dataset.
Response: We have contacted the MOSAiC team and we will have to wait for quite long for the processing of the data, however, as we mentioned above, thanks for all snow scientists who are willing to share the valuable dataset, we have collected enough campaign data for an extended validation.

We also add the comparison over Greenland with the retrieval from OLCI (Kokhanvosky et al., 2019) in the revised version. However, SSA retrieved in Kokhanvosky et al. (2019) used the simple relationship between SGS and SSA, that is $SSA = \frac{3}{\rho \times SGS}$, ρ is the bulk ice density. Even the SGS is perfectly retrieved, the calculation using this simple "conversion" may provide 20% error, and the SSA-albedo relationships limits the accuracy of SSA retrievals from albedo when the grain shape is unknown (Picard et al., 2009). We believe that our work is a new attempt to provide the information we are lacking now, that is we retrieved an "effective particle shape" and SGS, and provide unique relationship between SSA and SGS.
For instance, in the case of convex faceted particles such as droxtal, solid column, and plate, the calculation of total area is straightforward and based on the Cauchy's surface area formula:

$$A = 4A_p. \qquad (1)$$

Taking into account that for selected SPS, one can find corresponding V and A_p in database given by Yang et al., (2013), we have the following results for SSA of such particles:

$$SSA = \frac{4A_p}{\rho V}. \qquad (2)$$

In this case a solid column includes two equal cavities in the form of a hexagonal pyramid and cannot be considered as convex particle. The aspect ratio of hollow column with the height, d, of hexagonal pyramid is given according to Yang et al., (2013) as:

$$\frac{2a}{L} = \begin{cases} 0.7, & L < 100\mu m \\ \frac{6.96}{\sqrt{L}}, & L \geq 100\mu m \end{cases}, \quad d = 0.25L. \qquad (3)$$

The volume of such hollow column is given by

$$V = V_c - 2V_p, \qquad (4)$$

where the volume of solid column, V_c, and a hexagonal pyramid, V_p, are,

$$V_c = \frac{3\sqrt{3}}{2}a^2 L, \qquad (5)$$

$$V_p = \frac{\sqrt{3}}{2}a^2 d. \qquad (6)$$

Thus, the volume, V, is

$$V = \frac{\sqrt{3}}{2}a^2(3L - 2d). \qquad (7)$$

Employing the relationship between d and L given by Eq (A4) and excluding a, we have

$$V = \frac{2.5\sqrt{3}}{2}a^2 L \begin{cases} m_0 m_1^2 L^3, & L < 100\mu m \\ m_0 m_2^2 L^2, & L \geq 100\mu m \end{cases}, \qquad (8)$$

where $m = \frac{2.5}{\sqrt{3}/2}$, $m_1 = \frac{0.7}{2}$, and $m = \frac{6.96}{2}$. For a selected volume, V, the length, L, is calculated as follows:

$$L = \begin{cases} [V / m_0 / m_1^2]^{\frac{1}{3}}, & V < V_{100} \\ [V / m_0 / m_2^2]^{\frac{1}{2}}, & V \geq V_{100} \end{cases}, \qquad (9)$$

where $V_{100} = m_0 m_2^2 100^2$.

Let us now calculate the area of each triangle side of the pyramid

$$S_t = \frac{a}{2}\sqrt{d^2 + \frac{3a^2}{4}}. \qquad (10)$$

The area of lateral surface of two pyramids is

$$S_p = 3a\sqrt{4d^2 + 3a^2}. \qquad (11)$$

And the total surface area of hollow column is given by

$$S = 6aL + 3a\sqrt{4d^2 + 3a^2}, \qquad (12)$$

where a and d should be expressed via L according to Eq. (3).
Having obtained the total area, one can calculate specific surface area

$$SSA = \frac{S}{\rho V}, \qquad (13)$$

For each pre-defined effective shape, such a solid derivation is provided in part 1.

Then the key issue becomes can we use the Yang shapes (effective particle shape) to re-produce the real snow properties, which is also raised in the next comment, and our answer is yes and please see detailed explanations and corresponding figure in the next comment.

The issue with respect to the definition of RMSE, is clearly explained in the specific comments later as well.

Picard, G., Arnaud, L., Domine, F. and Fily, M., Determining snow specific surface area from near-infrared reflectance measurements: numerical study of the influence of grain shape, Cold regions and science and technology, 56, 10-17,2009

The grain shape is a big issue of this study. It is claimed to be a major advantage compared to other algorithms (e.g. L617) but the demonstration is missing. First be-cause it is difficult if not impossible to validate. I acknowledge that snow shape is a difficult topic. However as for the validation of the grain size, the choices of the authors are limiting the ability to perform the validation. The algorithm assumes and retrieves geometrical shapes that are representative of precipitating crystals, not of snow on the ground although the algorithm is supposed to be used for snow on the ground. A first consequence is that the algorithm can not perform well, because the phase function of such shapes does not apply to snow on the ground (expect for fresh snow). Snow on the ground is usually more rounded and irregular than crystals in the atmosphere. The second consequence (and the main one) is the difficulty to perform the validation. Data recorded by snow practitioners and scientists in the field usually follows the international classification of seasonal snow on the ground (Fierz et al. 2009, not cited in the manuscript) which has some shortcomings but is widely used. Since the algorithm does not use these “standard” shapes, it is inherently impossible to perform a fair comparison with external data. It follows a third consequence about the usefulness of the shape information retrieved by the algorithm. I’m wondering how useful is this retrieved “grain shape” for snow community since it does match with its standards. I suggest that to solve this major issue, ideally by adapting the shapes used by the algorithm, and if not possible at least by establishing a link between the different shape systems. Even if imperfect and highly uncertain, this link will benefit to the whole clarity of the paper and will help to shorten the validation section (see comments below). They should also explain why retrieving the shape is useful for the algorithm. The algorithm uses a first guess grain size from another algorithm but no comparison is given. I would expect the authors to demonstrate that taking into account the grain shape has an effective positive impact on the SSA or grain size estimates. This would be very useful for the snow remote sensing community to know if such an approach is fruitful.

Response: We agree that it is not possible for an apple-to-apple validation for the snow grain shape, as we discussed with Dr. Ghislain Picard by emails. Dr. Ghislain Picard also mentioned the way without an assumption of grain shape, that is to use an assumption of stochastic medium, consisting of irregular ice grains and air bubbles, however, in this manner, there is also parameters which cannot be validated. In particular, this is the mean photon path length. It is worth to notice that, all manners, for the retrieval of snow properties from satellite, needs to make some assumption, which is fundamentally needed for a specific retrieval algorithm (Langlois et al., 2020). We extend our introduction part to make a clearer statement in the revised version.

For the widely used ART model (the one used in the retrieval of OLCI in Kokhanovsky et al., 2019), even though the users do not highlight the issues linked to snow particle shape, these issues exist. (1) The original ART model (Zege et al., 2004; Kokhanovsky and Zege et al., 2005) is derived based on the assumption of second-generation fractal for ice crystal shape. (2) In the updated ART model (Kokhnaovsky et al 2018), g and B parameters are introduced. The g parameter depends on both size and shape. The B parameter depends strongly on the shape (Libois et al., 2014). Even one can state that the g and B parameters can be fitted to real observations, several issues linked to the assumption of particle shape occur (1) the accuracy of use single g parameter to describe the complicated particle phase function needs to be checked; (2) ART model is designed for medium with weakly absorption properties, thus it cannot be used for certain particle size/shape, especially for long wavelength, e.g. 1.6 μm. So, we cannot really avoid making certain (explicit or hidden) assumptions of SPS if it is not iteratively retrieved in the algorithm, like in our case.

To "demonstrate that taking into account the grain shape has an effective positive impact on the SSA or grain size estimates", the mathematical derivation (see example above) is included in part 1 and corresponding sensitivity study is also performed, in the revised version.

The question with respect to if the recent development from Yang can be used for the description of snow properties, such as the snow phase function, this has been confirmed by recent publications (e.g Saito et al., 2019; Pohl et al., 2020; Mei et al., 2021) and private communication with Prof. Ping Yang's group. We have included a detailed explanation in Part 1 and we will make a short summery of this issue in Part 2 as well. Additionally, we have compared the model from Yang with real surface BRDF measurements, including ground-based measurements, aircraft measurements and satellite observations, all shows that Yang shapes can provide good accuracy to simulate snow directional reflectance (Mei et al., 2021), which is the fundamental basis of our retrieval algorithm. Fig. 2 shows an example of how Yang database can re-produce the NASA Cloud Absorption Radiometer (CAR) instrument observed snow BRDF at the flight height of 200 meter, we will include some of our latest investigation in the revised version as well.

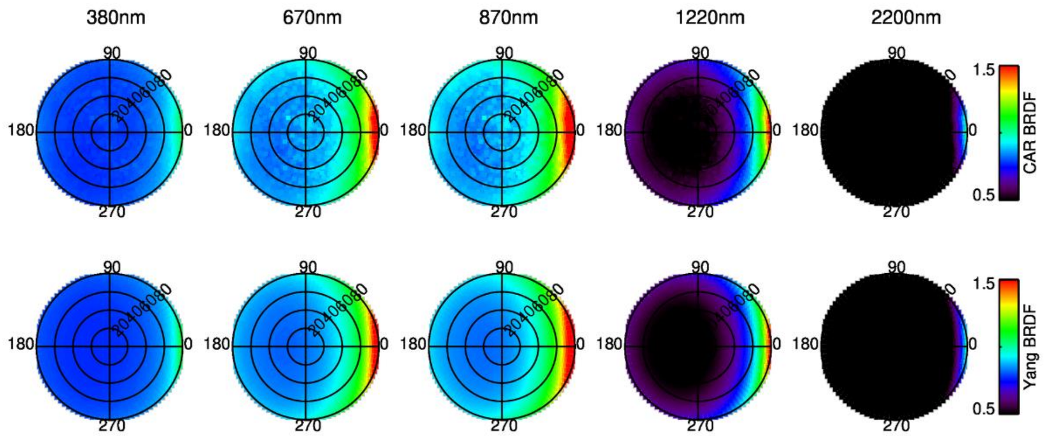

Fig 2 Comparison of NASA CAR instrument observed snow BRDF (upper) and Yang shape simulated snow BRDF (lower) for different wavelengths.

In short, the Yang et al. database can be used to describe the ice crystal local optical properties of snow.

With respect to the classification referring to Fierz et al. (2009), as clearly stated in the document, "we expanded and clarified where necessary but did not include those most recent developments that are not fully agreed upon by the whole community." And as far as I understand, the classification is a work to provide "the creation and maintenance of a common language", no local optical properties are available for the proposed names/classifications. And what we need is the local optical properties for an “effective particle shape” for the RTM calculations. We will emphasize that we should not over-interpret the shape we retrieved in the revised version.

However, we will include certain suggestion of the linkage between Yang’s shape and the shapes proposed in Fierz et al. (2009), as suggested by Dr. Ghislain Picard. We are currently harmonizing this issue with Yang’s group.

Fierz et al. (2009)		Yang et al (2013)
Precipitation Particles		Aggregate of 8 columns
Machine Made snow		Droxtal
Decomposing and Fragmented precipitation particles		Hollow bullet rosettes
Rounded Grains		Hollow column
Faceted Crystals		Plate
Depth Hoar	?	Aggregate of 5 plates
Surface Hoar		Aggregate of 10 plates
Melt Forms		Solid bullet rosettes
Ice Formations		Column

We believe that the only way to check the accuracy of a retrieval algorithm is comparison with independent ground-based measurements for parameters such as SGS and SSA, so in our revised version, with such a large validation samples, we will have a comprehensive understanding of the accuracy of XBAER algorithm.

Fierz, C., Armstrong, R.L., Durand, Y., Etchevers, P., Greene, E., McClung, D.M., Nishimura, K., Satyawali, P.K. and Sokratov, S.A. 2009. The International Classification for Seasonal Snow on the Ground. IHP-VII Technical Documents in Hydrology N°83, IACS Contribution N°1, UNESCO-IHP, Paris.

Langlois, A., Royer, A., Montpetit, B., Roy, A., and Durocher, M.: Presenting Snow Grain Size and Shape Distributions in Northern Canada Using a New Photographic Device Allowing 2D and 3D Representation of Snow Grains. Frontiers in Earth Science, 7. doi:10.3389/feart.2019.00347,2020

Mei et al., A new snow bidirectional reflectance distribution function (BRDF) model in the spectral region between UV and SWIR, in preparation, 2021

the benefits to split the study in two parts is not clear. The paper (part 2) presents the validation of an algorithm that is not described, which raise several questions and make it be difficult to read without reading the other paper (part 1). For the review, I didn't read the part 1 (I just browsed it) to be in the same position as a normal reader. I found that reading part 2 was difficult with many open questions about the algorithm and was sometimes annoying because of a few elusive statements referring to the part 1 without providing information. E.g. "The similarities and differences of the required snow parameters and their accuracy between the snow remote sensing community and other communities (e.g. field-measurement community) are detailed discussed in part 1 of the companion paper (Mei et al., 2020), thus we will not summery again in this paper. ". The length of this part 2 is normal and the information density is relatively low. For the comfort of the reader, I suggest to shorten or remove some sections (e.g. the first results section on Greenland), and merge with the part 1. Only if extending the validation as proposed above with a complete dataset and with Mosaic data, it would be justified to make two papers.

Response: We believe that with comments from reviewers of both part 1 and pat 2, for the revised versions, it is better to keep the two parts separated. The reasons are below:

Besides changes/updates on the current content, the reviewers of Part 1 suggest two more valuable sensitive study, which will further extend the length of the paper. In particular, the new sensitivity study includes

(1) Impact of spectral response of the two channels at 0.55 µm and 1.6 µm

In the revised version, one more section to investigate the impact of spectral response of the two channels at 0.55 µm and 1.6 µm is included. The following figure shows the spectral response functions for 0.55 µm (left) and 1.6 µm (right). Using these spectral response functions, we will perform the forward simulation with SCIATRAN model, to get TOA reflectance at 0.55 and 1.6 µm. After that, the retrieval using the XBAER algorithm will be performed. Since in the XBAER algorithm, we did not take the spectral response functions into account, thus this investigation shows the impact of the spectral response function on the retrieval results.

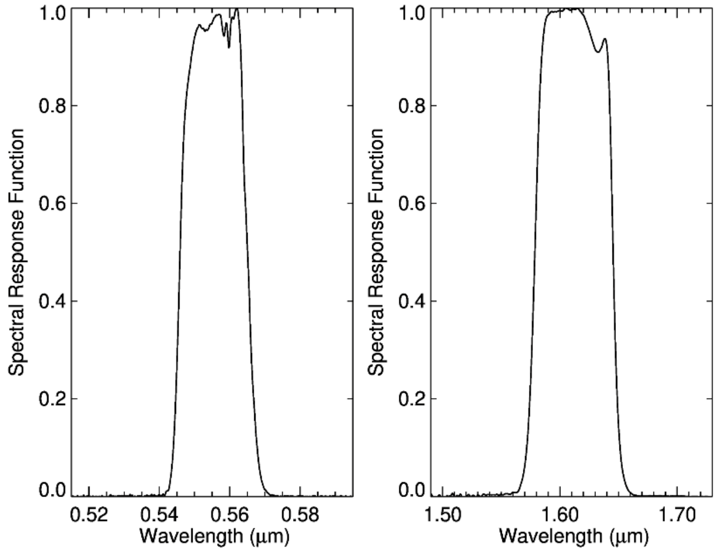

Fig. 3 Spectral response function of 0.55 (left) and 1.6 (right) μm of the SLSTR instrument

(2) The impact of snow profiles and mixture of different snow shapes

In order to assess the impacts of snowpack vertical inhomogeneity and the habit mixture on the accuracy of the retrieval algorithm, we add a new section in the revised version. The forward simulation of TOA reflectance at 0.55 and 1.6 μm will be performed using the vertical profile of grain size, particle size distribution, and habit mixture as presented in the following figure. The snow grain size profile was obtained during the SnowEx17 campaign (panel (a)). The particle size distribution of the ice crystal and the habit mixture are provided by Satio et al (2019) (see panel (b) and (c)). Then the retrieval will be performed assuming that the snowpack is vertically homogeneous and consisting of mono-disperse snow particles of single shape, and the retrieval accuracy will be assessed.

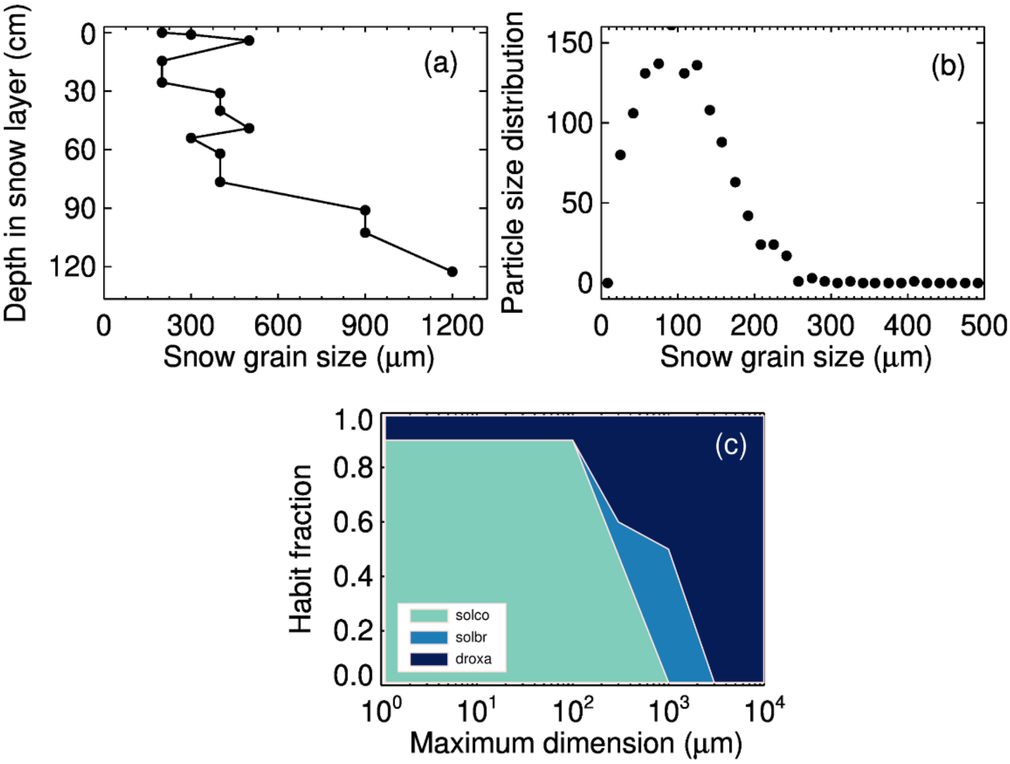

Fig. 4 Snow properties used for simulations to investigate the impacts of snow profiles and mixture of different snow shapes on XBAER retrieval (a) snow grain size profile observed during SnowEx17 (b) particle size distribution of snow grain size (c) ratio of snow particle shape. (b) and (c) are suggested by Saito et al (2019)

Saito, M., P. Yang, N. G. Loeb, and S. Kato: A novel parameterization of snow albedo based on a two-layer snow model with a mixture of grain habits, J. Atmos. Sci., 76, 1419–1436, 2019.

And at the meantime, as we mentioned, the validation is also largely extended using almost all available campaign data during 2016 -2020. We believe this extension will satisfy Dr. Ghislain Picard.

We think we always need to make a balance between the overlap content of such companion papers. We have also made a search on snow-topic-related journals, companion papers occur not so often in ground-based community, but very often in the satellite community. For a new retrieval algorithm, a comprehensively theoretical sensitivity study is essentially needed before the retrieval and evaluation of the retrieval results. We will, of course, harmonize again of the overlap content between these two parts. We will make a short summery of the content from part 1, if needed in part2, rather than use “see part 1”.

So, in short, we update both parts, by adding new investigations/validations. And we believe that keep them separated is an optimal way, taking both the content and the length into account.

Detailed comments:

L63. What is the definition of "grain size" used here ?

Response: grain size (effective radius) is defined as $3V/(4A_p)$, where V and A_p are the volume and average projected area, respectively.

L 69: correct "detailed discussed"

Response: Done

L70: "summery" → "summary"

Response: Done

L91-L92: I'm not sure to understand "to be with good quality"

Response: "to be with good quality" refers to "the retrieved plane albedo was compared with the measured spectral albedo and a good agreement was obtained with ±10%", stated in the cited paper. We update some details in the revised version.

L98-L99. Please add a reference / name for the operational product.

Response: The product is named as SGSP, which, together with the reference, is included in the revised paper.

L104 I'm not sure to understand "to partly taking snow irregular ".

Response: We removed this sentence in the revised version.

L118: "Details of these issues have been discussed in Part 1 of the companion paper.". Please remove and add a proper reference. Or just remove.

Response: We made a short summary of relevant content from part 1 to part 2.

L120-122: This sentence is strange, "no publication. . . especially using" seems contradictory.

Response: We have updated this sentence in the revision.

L 124-126. I don't understand the sentence. What is an "optimal complex shape". The part 1 paper seems to use very geometrical/simple shapes and the goal of the retrieval algorithm is to retrieve SPS. How does this apply to this sentence ? Also, what do you mean by the e.g. TOA ?

Response: "optimal complex shape" is the shape for which the difference between simulated and measured reflectance is minimal. That means, we need to pick up 1 "optimal complex shape" from the 9 "candidate shapes".

TOA, as we mentioned in the manuscript, is the Top Of the Atmosphere, the TOA reflectance or radiance is the quantity observed by satellite, which is used later for our retrieval.

We believe the word "complex" is misleading and we deleted this word in the revised version.

L147-149. I suggest to move this statements to the conclusion.

Response: Done

L150. I suggest to remove this statement or merge the two papers.

Response: We included a short summary in part 2 of "the three points we mentioned in Part 1".

L152 – L162. I suggest to move this paragraph to the discussion because it is a typical analysis of the uncertainties of the results/validation. The representativeness issue is a general problem, that affects any in-situ vs remote sensing comparison. Why the SPS would be particular? This also concerns SGS and SSA.

Response: According to our previous experience with non-experts or even experts for the discussion of the comparison between ground-based measurement and satellite retrievals, it is worth to put some general description as we are doing now, in the very beginning of the paper. The "scale issue" can be more than a "general" problem because this fully depends on your retrieval parameters, especially on the "inhomogeneity" of your retrieval parameters.

We had a long discussion with Dr. Joshua King, and we include an investigation of this issue using the observations over tundra basin. The measurements over tundra basin provides the possibility for such an investigation.

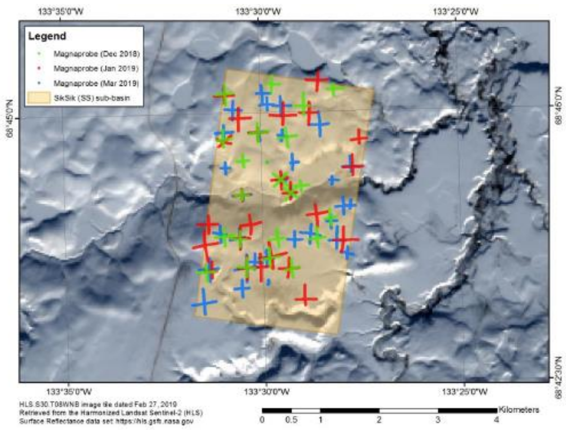

Campaign Totals
Snow pits: 80
Snow depths: 21946
SnowMicroPen: 1444

	Static	Roving	Total	$\overline{AT}$ [°C]	Crew [#]
November	6	16	22	-20.0	3
January	6	19	26	-28.4	4
March	6	26	32	-8.3	5

Fig. 4 Information of measurements over tundra basin (provided by Dr. Joshua King)

L170. Remove double “show”.

Response: Done

L215. I suggest to remove SnowEx17 grain shape from the table because it is misleading even with the warning in the legend caption. Instead it is possible to list these grain type in the caption and/or in the main text. Note that the grain type measured by SnowEx17 are not specific to this campaign but refer to the international classification (Fierz et al. 2009).

Response: We think the information of SnowEx17 in this table help the readers for a better understanding of the analysis later. We would like to keep it in Table 1. And we update this table by adding possible suggestions of the linkage between Yang shape and the shapes proposed in Fierz et al. (2009). We are currently discussing it with Prof. Ping Yang’s group.

L253 have→are

Response: Done

L276. Could you give a definition of spherical albedo and Lambertian surface albedo ?

Response: The Lambertian surface albedo is defined as the ratio of reflected to incident flux.

The spherical albedo is the fraction of the incident solar radiation diffusely reflected over all directions (albedo of an entire planet).

We include some explanation in the revised version.

L281. Could you indicate the resolution of MERRA ?

Response: MERRA resolution is 1°×1°

L282. Our → a

Response: Done

L339-355. The comparison is very qualitative and referring to generic and broad "classification" of "polar snow" does not bring significant information for this validation, especially because not all the existing references about snow grain shape and size have been taken into account. It must be taken into account that July is warm with a large proportion of the ice-sheet subject to melt, which unequivocally leads to rounded coarse grains very quickly.

Response: We largely extend the validation, as we mentioned above. Some measurements will include more information of the shape information, for instance, the aspect ratio of the ice crystal particle. We also highlight that the reader should not over-interpret the retrieved shape.

The impact of temperature on shape is included in the revised version.

Because the validation can not be done with information that are not available, I suggest to convince the reader that the results are plausible using cross-analyzed external data: use MERRA to separate where the snow is fresh and for which the present discussion in these lines apply fairly well.

Response: We include the cross-validation in the extended validation. And a post-processing to remove "ice and dirty snow" is also be introduced in the additional runs.

Where snow is fresh use successive image to show that SGS increases (and SSA decreases) as predicted by metamorphism (as you suggest, July is interesting for the most rapid metamorphism). use passive microwave (or MERRA or SLSTR thermal channels) to separate where melt is active and where the grains are very likely to be rounded. - use the images next 28 July 2017 to demonstrate that the blue shape for instance in NW Greenland are not due to clouds/aerosols. (I've made this comment before reading the discussion, see further comments below).

Response: We include the above suggestion with respect to the explanation into the revised version.

I also suggest to mask out areas in the ablation zone with ice and dirty snow, as the algorithm does not work in these cases. This should be emphasized.

Response: We include post-processing to remove "ice and dirty snow" in our additional runs.

Fig 3. adding a scatterplot with relevant statistics (R^2, RMSE, bias, . . .) is common

for a more quantitative validation. In particular, it would be useful to compute the same statistics with the first guess to really show the benefit of the algorithm.
Response: Scattering plot with relevant statistics is used in the extended validation. We also include these parameters from the first guess in our revised version.

L371. The previous section was titled "Results" but was also a comparison (and validation to some extent). Why not a unique Result section that includes both comparison?
Response: Done

L372. I suggest to remove "validate".
Response: Done

L373. ground-based/aircraft → ground-based and aircraft
Response: Done

L377- 379. I'd remove this introductory sentence that starts by concluding that the algorithm is good although the actual goal of the present sessions is to perform the validation.
Response: Done

L 385. "time and location" or "times and locations".
Response: times and location

L394. Why the rows are not sorted chronologically as in next figure ? What is the order? Has the gray shade in the last row a meaning ?
Response: We have sorted chronologically as in next figure in revised version. We have removed the gray shade in the revised version.

L398. This is the second "Fig 4". Review numbering. +Please add a scale to the maps.
Response: We have harmonized the figure number and put the scale on the maps in the revised version.

L406. How does this perform in the case of thin clouds ?
Response: There will be risk of remaining cloud contamination in the retrieval.

Fig 4 and Fig 5. I don't understand why two figures ? If I understand well, Fig 4 is a zoom of Fig 5 ? They should be merged in a single composition using the same symbology / graphic style.
Response: We have merged Fig. 4 and 5 in to one figure in the revised version.

L412-413. “is not correctly avoided”. This is a bit confusing. The next sentence is clearer to me but seems to be in contradiction with Table 3 indicating “cloud contaminated snow” for this date (which seems accurate based on Fig 4).

Response: We have updated the order and explanations of Table 3. The sample of 9 Feb. (partly cloudy) is not detected by the cloud screening while the sample of 11 Feb. has been detected, however, to check the impact of cloud contamination, we have manually “removed” the cloud screening for sample 11 Feb.

L388 indicates that the comment in Table 3 is obtained with the algorithm. Please clarify.

Response: Done

L413. Give → gives.

Response: Done

L421. Add a ref to the study.

Response: Done

L442. “Our → a” or “our calculations with”

Response: Done

L444. Fig 1 → fig 1 with a lowercase as it is referring to another paper. Add the ref.

Response: Done

L451-452. “cloud effective radius” → “cloud ice crystal effective radius”. SGS and “ice crystal size” are used interchangeably in the paper which is sometimes (and especially here) confusing.

Response: We harmonized the names in the revised version.

L464. “”This is similar to the issue in field measurements.” what do you mean ?

Response: For the field measurement of SSA, certain shape assumption is also used, and the assumption may not exact occur as well.

Leppanen, L., Kontu, A., Vehvilainen, J., Lemmetyinen, J. and Pullianinen, Comparison of traditional and optical grain-size field measurements with SNOWPACK simulation in a taiga snowpack, Journal of Glaciology, 61, 151-162, 2015

Langlois, A., Royer, A., Montpetit, B., Roy, A., and Durocher, M.: Presenting Snow Grain Size and Shape Distributions in Northern Canada Using a New Photographic Device Allowing 2D and 3D Representation of Snow Grains. Frontiers in Earth Science, 7. doi:10.3389/feart.2019.00347,2020

L465. " (e.g.,the measurement of SSA),". This is generally not true. Do you refer to a precise device and processing?

Response: Yes, this depends on the device and how the measurements are obtained, we include this explanation in the revised version.

L466-470. I'd suggest to define in the method section (Table 2) the most-likely correspondence between Yang's shapes and the snow type defined in the international classification (that used in SnowEx) so it is possible here and in the Section 4 in the results section to assess the algorithm performance in a more rigorous way.

Response: Firstly, we try to make possible linkage between Yang shapes and the "international classification". Secondly, other campaigns (such as campaign performed in China) provide some information with respect to the aspect ratio of particles, which is used to quantify the "accuracy" of shape as well. But again, we would like to highlight that we should not over interpret the retrieved "effective particle shape".

L473. "A previous publication" or cite more than one

Response: Done

L474 are → is

Response: Done

L479 "is 'facet' while XBAER says 'droxtal' both tend to be roundish". Facets according to Fierz et al. 2009 is not rounded. If the retrieval algorithm SPS can not distinguish rounded grains from faceted grains because both are droxtal, how useful it this for field practitioners ? This asks an important question that is not addressed in the introduction: why and for what usage to retrieve SPS from satellite ?

Response: We try to make a linkage between Yang's shape and shapes defined in Fierz et al. (2009). And we will highlight that we should not over-interpret the retrieved SPS in the revised version. The retrieved SPS is an "effective shape", which provides the best agreement between radiative transfer simulations and satellite observations.

As we mentioned above, SGS and SPS are the two fundamental inputs for the RTM calculations in XBAER algorithm.

Additionally, with the extended comparison, we will focus more on the validation of SGS and SSA, in the revised version. The comparison of SPS will be reduced.

L483. I do not agree. It is also believed that grains get rounded due to sublimation in blowing snow (Domine, 2009). This probably depends on the conditions, on the actual grains available on the surface, and the strength and duration of the saltation/reptation process.

Response: We have updated this statement in the revised version.

L493-496. Please indicate the number of points of each comparison (n=...) and the statistical significance of the results. By “difference” do you mean “rms difference” or “difference of the average” ?

Response: Number of points will be included in the extended validation.

“difference” means “difference of the average”

L548. Here it would be particularly interesting to see how good the first guess predictor of SGS. I’m really interested by knowing if the algorithm sophistication is worthwhile.

Response: We include a small validation/analysis of the accuracy of the first guess.

L533. I’m not sure to understand how the RMSE is calculated. The RMSE includes both systematic and random errors, and here given the difference of the mean, the RMSE should be at least 165 – 138 = 17 microns while the text indicate 12 microns. Please check also “lower grain sizes”.

Response: The definition of RMSE is calculated for two groups (satellite retrievals and corresponding SnowEx measurements), not for one group. The understanding reviewer mentioned above is to calculate RMSE for a single group, which indicates the “scattering properties” of this group of data. In our manuscript, RMSE is calculated as following:

$$RMSE = \sqrt{\frac{1}{N}\sum_{n=1}^{n=N}(SSA_n^{XBAER} - SSA_n^{SMART})^2},$$

where N is the number of samples, SSA_n^{XBAER} and SSA_n^{SMART} are the SSA of sample n obtained from XBAER and SMART retrievals.

L550. The same question applies for SSA, with a difference in the mean of 3 m2/kg, it is not possible that the RMSE is 2 m2/kg.

Response: See above

Fig 8. This figure is interesting but should be used earlier in the validation to infer the errors of estimations. I see the following possible artifacts: - The presence of undetected clouds in the NW Greenland. - The dramatic grain size decrease after 28 July in Eastern Greenland (analysis around L588) is very suspicious and stronger evidences are needed to prove that it would be related to a massive drift event, and not to a retrieval artifact. In particular it would be necessary to demonstrate that the wind sustained over 6m/s for a sufficient long period of time to really bring sufficient quantities of small grains over the considerable distance. - Why grain shape changes so fast between a Droxtal to a column in central Greenland ? Wind is able to drift fresh snow, but in the absence of recent snowfall, if snow was already Droxtal at the surface, wind can not transform it into more elongated crystals. Faceting of grains at such a pace is suspicious. - The Western side is also affected by the grain size change. The shape change is also marked and different from that observed in the Eastern side. Why this is not discussed?

Response: We have included more explanations for Fig.8, especially with the information of wind from ECMWF. The possible reason of blow of fresh snow due to wind or ice crystal change due to temperature are further analyzed.

L590. The weblink does not point to any data. A figure should be added in the supplementary with direction and wind speed.

Response: We have included the wind information from ECMWF in the revised version.

Dear Editor, dear reviewer,

Thanks for the valuable comments, which help to improve the quality of the paper. The detailed replies are addressed below point by point in blue. The key issue raised by reviewer is we need more validation. The following table shows the update of validation in the revised version.

	Current version	**Revised version**
Number of site(s)	1	7
Total observation length	1 month	~10 years

Best regards,

Linlu Mei on behalf of all co-authors

General Comments

This paper describes the results and validation of the XBAER algorithm that retrieves snow grain size (SGS), specific surface area (SSA), and particle shape (SPS) from Sentinel-3 SLSTR instrument. The paper presents the results and evaluate them using the MODSCAG product, in-situ measurements from SnowEx17, and airborne-based retrievals. The validation for cloud-free and partial cloud cover shows promising results from the XBAER algorithm; however, there are some issues related to the validation process and the paper's writing structure.

Response: The validation is largely extended by including all possible existing campaign during 2016-2020. The analysis, including the writing structure is also re-ranged. The extended dataset for validation is shown in the figure below

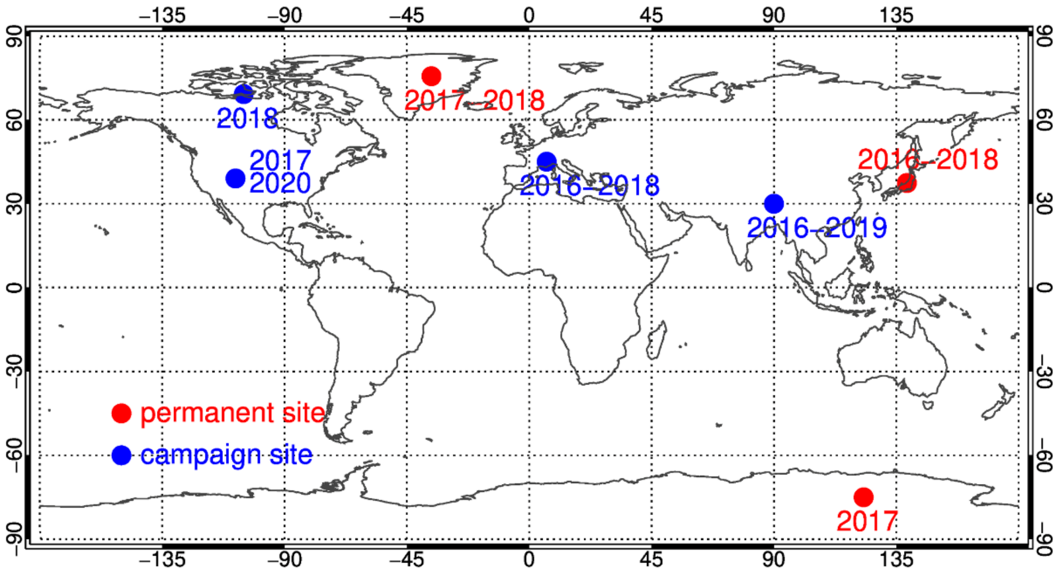

Fig. 1 Geographic distribution of the validation sites. The colors represent the type of each site while the observation period used in this manuscript is indicated near each site.

Regarding the validation process, the main negative point is that the authors state that these are preliminary results and that they are waiting for more data from the MOSAiC project to increase the number of observations for validation. However, this paper accompanies another paper on the development of the XBAER algorithm. If these are preliminary results, it would make more sense to fit some of these results in the first paper, and then wait for the MOSAiC data to submit a more comprehensive validation in the second paper. I understand that it is hard to obtain enough data for remote sensing validation, but since there is ongoing data collection, the wisest decision will be to wait until the MOSAiC dataset is fully collected.

Response: Beside the extended validation dataset above, we have also contacted the MOSAiC team, however, the latest information is that we properly have to wait quite some time for the dataset, and we believe that the extended validation is enough for a comprehensive understanding of XBAER algorithm. We will move the content with respect to the MOSAiC comparison in the summery part to indicate our future work.

Regarding the paper's writing structure, in general, the paper lacks conciseness. A few general comments about this topic are the following: - There are long sentences on multiple occasions. - The authors should be more careful about using quantitative adjectives when describing their results or other authors' results. I would recommend using the actual number instead. - I would suggest that the authors make a thorough revision of the use of articles, prepositions, and verb agreements in the paper. - The purpose of this paper should be more clearly stated in the introduction. - There is excessive use of quotes. - The discussion paragraph is too long and speculative. There is a lot of discussion in the results section already. I would recommend the authors to create a section for results and discussion together instead. - The conclusion is too long and with too much redundancy. It should state the main findings, limitations, and future studies, and if it was able to meet the goals of the study. In addition, the main findings in the conclusion should follow the same order that the results are presented.

Response: We have thoroughly improved the presentation in the revised version. More specifically (1) We have updated the introduction part; (2) We have cut long sentences into short ones; (3) we have fixed possible grammar issues (4) We have merged section 4 and 6 to create a "result and discussion section" (5) We have shorten the conclusion part, with the same order as that the results are presented

More detail is provided in the Specific Comments and Technical Corrections sections below.

Other general comments on the scientific soundness of the paper are the following: How have you dealt with the forest in the Grand Mesa site? - One way to improve the SGS validation would be perhaps to extend the validation using more MODSCAG scenes.

Response: We have performed the simple collocation, according to our understanding, the impact of the forest within an SLSTR pixel is mitigated due to the usage of "effective Lambertian albedo". We include MODSCAG for the SnowEx17 validation in the revised paper.

It is not appropriate to use full cloud cover field measurements to validate a remote sensing retrieval that only works with cloud-free conditions. Using partially covered skies might still be a reasonable assumption, as long as the limitations of the retrievals under these conditions are addressed, but not full cloud cover as on Feb. 11, 2017. Retrieving snow properties for full cloud cover only shows that your model is able to characterize the properties of cloud ice crystals, but that has no implications for snow properties on the ground.

Response: With the largely extended validation, this issue will not be so critical. However, we believe that the validation using the fully cloudy scene is also helpful. We have presented our results in the Sentinel 3 validation meeting held last month (hosted by ESA/EUMETSAT), and most snow scientists show great interest to see how we can avoid a pre-cloud-identification in our snow retrieval because cloud screening above snow always brings large uncertainties in the dataset.

Specific Comments

Line 14: The OLCI instrument was not used directly to retrieve snow properties; therefore, it would be better to only mention it when talking about the cloud screening process.

Response: We removed OLCI here

Line 52: Melting snow does have lower albedo, but the main mechanism that decreases albedo is actually the absence of snow cover.

Response: We updated this sentence in the revised version.

Line 62: The terms field- based and in-situ are synonyms; there is no need to use them together.

Response: We removed field-based in the revised version

Lines 62 to 67: Consider splitting or rearranging this sentence to improve its clarity.

Response: We updated this sentenced and spitted in the revised version.

Line 82: When you mentioned snow fraction. Did you mean snow cover fraction?

Response: Yes, snow cover fraction

Line 100: You should drop "imagery" if you are talking about instruments. You should also add one space before "(EO-1)" in the previous line.

Response: Done

Line 104: I would rewrite this sentence as: "to partly take into account irregular shape impacts on snow reflectance".

Response: Done

Lines 106 to 108: I am not sure if this information is relevant in this paragraph.

Response: We believe it fits here because it gives the reader an overview of the change of SPS with respect to meteorological conditions.

Lines 108 to 109: It is unclear what the classification system is for. Is it for classifying SPS? If yes, it would be a good idea to specify that and explain how the system classifies SPS.

Response: We extended the explanation of the classification of snow from Kikuchi et al (2013) in the revised version.

Lines 130 to 131: In this sentence, the last "retrieval" is redundant. For the sake of

conciseness, try to avoid doing this in other sentences of the paper.
Response: We have checked thoroughly of this presentation-related issues and ask our native speaker to double-check as well.

Line 150: Try to be more specific when mentioning pieces of the part 1 paper. You could maybe mention the section number to help the reader find it in the other paper.
Response: We have made a short summery of information from Part 1, if needed in part 2, rather than use "see part 1" in the current form.

Line 152: I would suggest changing the title of the point to: "Difference between field-measured and satellite-derived SPS".
Response: Done

Line 183: The acronym BRDF was not introduced in the text yet.
Response: It is introduced in the revised version.

Line 189: Try to be consistent with the terminology. I have seen in-situ, field-based, field-measured, and ground-based, used interchangeably. Better if you choose the most appropriate and use it consistently throughout the text.
Response: We harmonized in the revised version.

Line 199: European Space Agency (ESA) was previously introduced.
Response: Removed

Figure 1: It would be good to add a picture of the Senator Beck Basin site as well. In the map, make sure to increase the font and include the name of the two sites. Ideally, it would be good to have an inset zoomed to the two sites together with the US map.
Response: We updated the figures according to the suggestion.

Table 2: I am not sure if the SnowEx17 column is necessary here, since there is no linkage to the Yang columns, and it was previously mentioned.
Response: Together with comments from reviewer 1, we included the classification system from Fierz et al. (2009) in Table 2. The SnowE17 is also based on the Fierz et al. (2009)

Line 239: The sentence "masking by gases and molecules" is not the most accurate. I would suggest changing it for "attenuation and scattering by gases and aerosols".
Response: Done

Figure 2: I would suggest trying to minimize the amount of text in this flowchart. Also, you would have to connect the two biggest green boxes inside the dashed line to represent

better that this is an iteration process.

Response: There is an arrow missing which should link the two green boxes.

As to the texts in the flowchart, since XBAER algorithm includes quite some other previous published algorithms, we would like to take the heritage of it.

Figure 3: I am impressed with the spatial detail of XBAER retrievals, but I noticed two geometrical-shaped features in Eastern Greenland. Could you please comment on why this is happening in that region?

Response: Thank you for the positive feedback of our retrievals. The two geometrical-shape features in Eastern Greenland are explained by the impact of large viewing zenith angle. This Figure is created by three SLSTR swaths, the two geometrical-shaped features occur at the edge of the middle swath (large viewing zenith angles). In XBAER, the "effective Lambertian albedo" assumption is used and this assumption will introduce error under large viewing zenith angle condition. We included the explanation in the revised version.

Line 336: This parenthesis is probably unnecessary: "(humidity, temperature, … etc.)".

Response: We removed it

Lines 336 to 347: I appreciate that you tried to compile as many studies as possible to perform a qualitative validation, but this section is too long. Instead of listing all the values, you can try to summarize what you found by the other authors focusing only on what you used for your validation.

Response: We reduced certain previous studies in this section, to make sure that only close-related publications are cited here.

Line 348: There is no need to use quotations here.

Response: We removed it

Figure 5: It seems that the legend of the cloud maps is wrong. It should be cloud (light blue) and cloud-free (white).

Response: The current legend is a little bit mis-leading, the "snow-free" legend refers to the area where XBAER retrieval is not performed, this includes (1) snow-free and cloud free (2) cloud above snow; (3) cloud above snow-free. The light blue is snow. We updated the legend in the revised version.

Line 529: I am not sure if time series would be the best term to describe this analysis. The Sentinel-3 image is a snapshot of time, while the aircraft surveying takes about 2 hours to complete. It would be better to relate this to space (coordinates), and probably some correction would be needed to address differences in solar zenith angle between the two instruments. Was that addressed? Differences in solar zenith angle can also represent different amounts of shadows, which might explain some of the differences between XBAER and SMART.

Response: We have published another paper for this topic (Jäkel et al., 2021), in which more detailed comparison between XBAER and SMART is given. We included some findings from the new publication in the revised version. Specifically, possible shadow effect on the retrieval accuracy is detailed discussed in the paper of Jäkel et al (2021).

Jäkel, E., Carlsen, T., Ehrlich, A., Wendisch, M., Schäfer, M., Rosenburg, S., Nakoudi, K., Zanatta, M., Birnbaum, G., Helm, V., Herber, A., Istomina, L., Mei, L., and Rohde, A.: Comparison of optical-equivalent snow grain size estimates under Arctic low Sun conditions during PAMARCMiP 2018, The Cryosphere Discuss. [preprint], https://doi.org/10.5194/tc-2021-14, in review, 2021.

Lines 533 to 534: The mean SGS from SMART is actually higher than for XBAER.

Response: We fixed this word in the revised version.

Lines 578 to 579: That depends on environmental conditions.

Response: We included more information for these sentences to clarify the dependent of length of time scale on environmental conditions.

Lines 587 to 589: It is unlikely that blowing snow would transport fresh snow from the ground to such long distances in such a short period.

Response: We included the ECMWF wind information in the revised version, and an updated explanation for this sentence will be included.

Line 636: There is extra space before the parenthesis. In addition, there is no need to repeat the ice crystal types in the conclusions.

Response: extra space before the parenthesis is removed and we have deleted the ice crystal types in the conclusion.

Line 656: It would be better to use “inversely correlated” than “anti-correlated”.

Response: Done

Technical Corrections

Line 54: Replace “of change snow properties” to “of snow properties change”.

Response: Done

Line 54: Replace “annular” for “annual”.

Response: Done

Line 60: Replace "temperatures surrounding" for "surrounding temperatures".
Response: Done

Line 70: Replace "summery" for "summarize".
Response: Done

Line 86: Replace "Jin et al (2008)" for "Jin et al. (2008)".
Response: Done

Line 90: Replace "usage" for "use".
Response: Done

Line 96: Replace "the in-situ measurement" for "in-situ measurements". This sentence would be clearer if you add a comma after Antarctica.
Response: Done

Line 114: Replace "e.g." for "e.g.,". This repeats a couple more times throughout the text.
Response: Done

Line 116: There is a missing space before the citation parenthesis.
Response: We have included a space

Line 182: Replace "SLSTR/AATSR" for "SLSTR and AATSR".
Response: Done

Line 217: There is a missing period. Also, you should replace "have not linkage" for "have no linkage".
Response: The problems are fixed and phase updated.

Line 226: Replace "is" for "was".
Response: Done

Line 233: Replace "present" for "presented", and add a comma after "(about 80° SZA)".
Response: Done

Line 263: Replace "details" for "detailed". Line 373: Replace "is" for "are".
Response: Done

Line 439: Should replace "the warmer conditions leads to" for "which leads to".
Response: Done

Line 527: Remove hyphen after "SGS".

Response: Done

Line 645: Replace "minimization" for "minimizations".

Response: Done

Line 671: Replace "usage" for "use".

Response: Done

The retreival of snow properties from Sentinel-3SLSTR~~/ Sentinel-3~~ - part 2: results and validation

Linlu Mei[1], Vladimir Rozanov[1], Evelyn Jäkel[2], Xiao Cheng[3], Marco Vountas[1], John P. Burrows[1]

[1] Institute of Environmental Physics, University of Bremen, Germany

[2]Leipziger Institut für Meteorologie, University of Leipzig, Germany

[3]School of Geospatial Engineering and Science, Sun Yat-Sen University, Zhuhai, P.R. China, 519082

Abstract

To evaluate the performance of eXtensible Bremen Aerosol/cloud and surfacE parameters Retrieval (XBAER) algorithm, presented in part 1 of the companion paper, this manuscript applies the XBAER algorithm on the Sea and Land Surface Temperature Radiometer (SLSTR) ~~and Ocean and Land Colour Instrument (OLCI)~~ instrument~~s~~ onboard Sentinel-3 and evaluates its performance. Snow properties: Snow Grain Size (SGS), Snow Particle Shape (SPS), and Specific Surface Area (SSA) are derived under cloud-free conditions. XBAER derived snow

properties are compared to other existing satellite products and validated by ground-based/aircraft measurements. Cloud screening is performed by standard XBAER algorithm synergistically using OLCI and SLSTR instruments both onboard Sentinel-3. The atmospheric correction is performed on SLSTR for cloud-free scenarios using Modern-Era Retrospective Analysis for Research and Applications (MERRA) Aerosol Optical Thickness (AOT) and aerosol typing strategy according to the standard XBAER algorithm. The optimal SGS and SPS are estimated iteratively utilizing a Look-Up-Table (LUT) approach, minimizing the difference between SLSTR-observed and SCIATRAN simulated surface directional reflectances at 0.55 and 1.6 µm. The SSA is derived for a given retrieved SGS and SPS pair. XBAER derived SGS, SPS and SSA have been validated using *in-situ* measurements from the recent campaign SnowEx17 during February 2017. The comparison of the retrieved SGS with the *in-situ* data shows a relative difference between XBAER-derived SGS and SnowEx17 measured SGS of less than 4%. The difference between XBAER-derived SSA and SnowEx17 measured SSA is 2.7 m^2/kg. XBAER-derived SPS can be reasonable-explained by the SnowEx17 observed snow particle shapes. An intensive validation shows that (1) For SGS and SSA, XBAER derived results show high correlation with field-based measurements, with correlation coefficients higher than 0.85. The Root Mean Square Error (RMSE) of SGS and SSA are around 12 µm and 6 m^2/kg ; 2) For SPS, aggregate SPS retrieved by XBAER algorithm is likely to be matched with rounded grains while single SPS in XBAER is possibly linked to faceted crystals.

The comparison with aircraft measurements, during the Polar Airborne Measurements and Arctic Regional Climate Model Simulation Project (PAMARCMiP) campaign held in March 2018, also shows good agreement (with R=0.82 and R=0.81 for SGS and SSA, respectively). XBAER-derived SGS and SSA reveal the variability of the aircraft track of PAMARCMiP campaign. The comparison between XBAER-derived SGS results and MODIS Snow-Covered Area and Grain size (MODSCAG) product over Greenland shows similar spatial distributions. The geographic distribution of XBAER-derived SPS over Greenland and the whole Arctic can be reasonable-explained by campaign-based and laboratory investigations, indicating reasonable retrieval accuracy of the retrieved SPS. The geographic variabilities of XBAER-derived SGS and SSA over both Greenland and Arctic-wide agree with the snow metamorphism process.

1 Introduction

Change of snow properties is both a consequence and a driver of climate change (Barnett et al., 2005). Snow cover and snow season, especially in Northern Hemisphere, are reported by different models, to decrease due to climate change (Liston and Hiemstra, 2011). The reduction of snow cover leads to the change of surface energy budget (Cohen and Rind, 1991; Henderson et al.,2018), a reduction of Asian summer rainfall (Liu and Yanai, 2002; Zhang et al., 2019), a loss of Arctic plant species (Phoenix, 2018) and other impacts on societies and ecosystems (Bokhorst et al., 2016). Snow may influence the climate through both direct and indirect feedbacks (Lemke et al., 2007). The direct feedback is the snow-albedo feedback and the indirect feedbacks are involved by atmospheric circulation. The snow-albedo feedback describes the mechanism that melting snow (the absence of snow cover), caused by global warming, reflects less solar radiation, and further enhances the warming (Thackeray and Fletcher, 2016). The snow indirect feedbacks describe the impact of ~~change~~ snow properties change on monsoonal and ~~annular~~ annual atmospheric circulation (Lemke et al., 2007; Gastineau et al., 2017). However, the snow cover may be declining even faster than thought due to large uncertainties of how models describe the snow feedback mechanisms (Flanner et al., 2011). The uncertainties to describe the snow feedback mechanisms are largely introduced by the uncertainties of knowledge of snow properties (Hansen et al., 1984; Groot Zwaaftink et al. 2011; Sarangi et al., 2019). Snow properties depend on snow age, moisture, and surrounding temperatures ~~surrounding~~ (LaChapelle,1969; Sokratov and Kazakov, 2012).

~~Even though m~~Model simulations and field-based ~~*in-situ*~~ measurements provide valuable information of snow properties~~, such as~~(e.g., Snow Grain Size (SGS), Snow Particle Shape (SPS), Specific Surface Area (SSA)) for the understanding of changing snow and its corresponding impact on climate change.~~,~~ S~~s~~atellite observations offer another effective way to derive those snow properties on a large scale with high quality (e.g. Painter et al., 2003; 2009;

Stamnes et al., 2007; Lyapustin et al., 2009; Wiebe et al., 2013). The similarities and differences of the required snow parameters and their accuracy between the snow remote sensing community and other communities (e.g. field-measurement community) are discussed in detail ~~detailed discussed~~ in part 1 of the companion paper (Mei et al., 2020d).~~, thus we will not summery again in this paper~~. In this manuscript, SGS (effective radius) is defined as $3V/(4A_p)$, where V and A_p are the volume and average projected area, respectively.

Different retrieval algorithms to derive SGS have been developed for different instruments. Airborne Visible / Infrared Imaging Spectrometer (AVIRIS) and Thematic Mapper (TM) onboard Landsat are pioneer instruments used for the retrieval of SGS (Hyvarinen and Lammasniemi,1987; Li et al., 2001). Painter et al. (2003,2009) retrieved SGS using AVIRIS and Moderate Resolution Imaging Spectroradiometer (MODIS) data, exploring the information from both visible and near-infrared spectral channels. There are several available satellite SGS products for MODIS (Klein and Stroeve, 2002; Painter et al., 2009; Rittger et al., 2013) and its successor, Visible Infrared Imaging Radiometer Suite (VIIRS) (Key et al., 2013). For instance, the MODIS Snow-Covered Area and Grain size (MODSCAG) product is created utilizing a spectral mixture analysis method based on prescribed endmember. The endmember is a spectrum library for snow, vegetation, rock, and soil (Painter et al., 2009). The MODSCAG algorithm can provide snow cover fraction and snow albedo besides SGS on a pixel base. Topographic effects in MODSCAG are not considered and the MODSCAG product tends to overestimate SGS (Mary et al., 2013). Other retrieval algorithms have also been designed for and tested on the MODIS instrument (Stamnes et al., 2007; Aoki et al., 2007; Hori et al., 2007). Jin et al. (2008) retrieved SGS over the Antarctic continent using MODIS data based on an atmosphere-snow coupling radiative transfer model. Lyapustin et al. (2009) proposed a fast retrieval algorithm for SGS at a 1 km spatial resolution using MODIS observations. The algorithm is based on an analytical asymptotic radiative transfer model. Negi and Kokhanovsky (2011) proposed the us~~eage~~ of the Asymptotic Radiative Transfer (ART) theory to retrieve SGS. The retrieved snow albedo and grain size from Negi and Kokhanovsky (2011) were validated and showed good accuracy~~to be with good quality~~ for clean and dry snow. However, potential problems have been reported for dirty snow (e.g., soot/dust contamination). The Snow Grain

Size and Pollution (SGSP) algorithm retrieves SGS and pollution amount based on a snow model (Zege et al., 1998), without a-priori assumptions on SPS (Zege et al., 2011). The SGSP algorithm has been validated using ~~the~~ in-situ measurements over central Antarctica, and an underestimation of SGSP-derived SGS was reported under a large solar zenith angle (Zege et al., 2011; Carlsen et al., 2017). The algorithm is currently implemented for the MODIS instrument and provides operational daily snow products (Wiebe et al., 2011). New instruments such as Earth Observing-1 (EO-1) Hyperion ~~imagery~~ and OLCI have also been used to derive SGS (Zhao et al., 2013; Kokhanovsky et al., 2019). The algorithm proposed by Kokhanovsky et al. (2019) is conceptually based on an analytical ART model, which estimates snow reflectance by given SGS and ice absorption (Kokhaovksy et al., 2018). The snow grains in the ART model are described as a fractal~~, to partly taking snow irregular shapes impacts on snow reflectance into account~~.

Snow particle shape is a fundamental parameter needed to describe snow properties (Räisänen et al. 2017). The SPS keeps relatively stable before falling on the ground under cold and dry conditions while it has large variabilities under warm and wet conditions (Dang et al., 2016). The International Classification for Seasonal Snow on the Ground (ICSSG) has groupped the SPS into nine main morphological shapes: Precipitation Particles (PP), Machine Made snow (MM), Decomposing and Fragmented precipitation particles (DF), Rounded Grains (RG), Faceted Crystals (FC), Depth Hoar (DH), Surface Hoar (SH), Melt Forms (MF), Ice Formations (IF) (Fierz et al., 2009). Another classification system, named as "global classification" has been proposed in Nakaya and Sekido (1938) and has been updated recently by Kikuchi et al. (2013). The "global classification" is obtained based on the SPS. The information in Kikuchi et al. (2013) is qualitatively used to understand the satellite derived SPS in this manuscript. Due to the complexity of the ice crystal shape, simplified ice crystal shapes, such as fractal (Macke et al., 1996; Kokhanovsky et al., 2019) and droxtal (Pirazzini et al., 2015), have been used in some satellite retrievals and model simulations. However, previous investigations show that non-fractal snow types occur more frequently in reality (Gordon and Taylo, 2009; Comola et al., 2017). Information of SPS, even limited or inaccurate, is extremly helpufl and urgently needed for a better understanding of different snow types (Picard et al., 2009). The widely used spherical shape assumption in field-based measurements (e.g., Flanner and Zender, 2006) is not optimal for satellite-orientated retrievals, because the spherical shape assumption can not produce the angular distribution of snow reflectance with required accuracy (Leroux and Fily et al., 1998; Jin et al., 2008; Dumont et al., 2010; Mei et al., 2021), which will introduce an unacceptable magnitude of uncertainty in the satellite retrieved snow properties. ~~Details of these issues have been discussed in Part 1 of the companion paper.~~ Some attempts to derive ice crystal shape in ice clouds can be found in previous publications (McFarlane et al., 2005; Cole et al., 2014). However, there is no publication with respect to the retrieval of ice crystal shape in the snow layer~~, especially~~ using passive multi-spectrum satellite observations. Although habit mixture models are preferable for the description of snow grain shapes (Saito et al., 2019; Tanikawa et al., 2020; Pohl et al., 2020), the information content from satellite observation is limited compared to field-based measurements. Thus, an optimal single ~~complex~~ shape, which provides the best agreement between simulation and ~~with~~ satellite observation (e.g. Top of the Atmosphere (TOA) reflectance) is also needed.

A few attempts have been proposed to retrieve SSA from space-borne observations. The retrieval of SSA is actually performed based on the pre-retrieved SGS with an assumption of a given known SPS. Mary et al. (2013) retrieved SSA over mountain regions using MODIS data, assuming a spherical ice crystal shape. The ~~retrieval~~ algorithm performs a topographic correction for the surface reflectance to achieve a better retrieval accuracy. The overall difference, compared to field measurements, is 9.4 m^2/kg. Xiong et al. (2018) retrieved SSA using a snow reflectance model. The model simulates the light scattering process using a Monte Carlo method and shows an improvement of bidirectional reflectance, thus a better retrieval accuracy of SSA, compared to the spherical assumption. The overall difference, compared to field measurements, is about 6 m^2/kg.

This paper, as the companion paper of part 1, applies the XBAER algorithm on Sea and Land Surface Temperature Radiometer (SLSTR) onboard Sentinel-3 to derive SGS, SPS and SSA. The general concept is to use the channels, which are sensitive to SGS and SPS, simultaneously. The channels used in XBAER algorithms are 0.55 µm and 1.6 µm. An optimal SGS and SPS pair is achieved by minimizing the difference of atmospheric-corrected directional surface reflectances between satellite observations and SCIATRAN simulations. SSA is then calculated based on the retrieved SGS and SPS. Nine predefined ice crystal particle shapes (aggregate of 8 columns, droxtal, hollow bullet rosette, hollow column, plate, aggregate of 5 plates, aggregate of 10 plates, solid bullet rosette, column) (Yang et al., 2013) are used to describe the snow optical properties and to simulate the snow surface reflectance at 0.55 and 1.6 µm. ~~XBAER-derived SGS, SPS, and SSA will be used to support the analysis of MOSAiC (Multidisciplinary drifting Observatory for the Study of Arctic Climate) expedition measurements.~~

As~~Besides the three points we~~ mentioned in part 1 of the companion paper, the nine Yang SPSs used in the XBAER algorithm is proven to be a new option to describe the ice crystal local optical properteis for the snow community (e.g Saito et al., 2019; Pohl et al., 2020; Mei et al., 2021), we would also like to emphasize several~~one~~ more point to avoid misunderstandings between different scientific communities.

- **Difference between field-measured and satellite-derived SPS~~A comparison between field-measured and satellite-derived SPS~~**. A field-measured SPS is an optical shape for a single ice crystal while satellite-derived SPS is an averaged radiative shape on a certain geographic area. The geographic area is determined by the instrument spatial resolution (1 kilometer as used in this study). Thus it is unreasonable to directly compare a kilometer average radiative shape to a single ice crystal shape. However, for a region with a similar snow metamorphism process (Colbeck et al., 1980;1983), the field measured SPS may provide some representative information with respect to if the ice crystal shape is convex (e.g. spherical shape) or non-convex (aggregate shape), which is also critical for further applications. This fundamental difference between field-measured and satellite-derived SPS restricts that only a qualitative evaluation of the satellite retrieved SPS is possible. Please be noted that this spatial resolution issue is more than just a typical "general scale issue" becuase it fully depends on the paramters retreived, especially on their inhomogeneity.

- **Requests to describe snow properties in the radiative transfer theory**: there is another way to describe snow properties in the radiative transfer theory. This manner needs no knowledge with respect to SPS, but use an assumption of stochastic medium. However, in this manner, there are also parameters (e.g. mean photon path length) which cannot be validated. It is worth to notice that, all manners, for the retrieval of snow properties from satellite, needs to make some assumptions. These assumptions are fundamentally needed for a specific retrieval algorithm (Langlois et al., 2020).

- **Different radiative transfer models used for snow community**: For the widely used Asymptotic radiative transfer (ART) model, even though the users do not highlight the issues linked to SPS, these issues exist. (1) The original ART model (Zege et al., 2004; Kokhanovsky and Zege et al., 2005) is derived based on the assumption of second-generation fractal for ice crystal shape; (2) In the updated ART model (Kokhnaovsky et al 2018), *g* and *B* parameters are introduced. The *g* parameter depends on both SGS and SPS. The *B* parameter depends strongly on SPS (Libois et al., 2014). Even one can state that the *g* and *B* parameters can be fitted to real observations, several issues linked to the assumption of SPS occur: (1) the accuracy of use a single *g* parameter to describe the complicated particle phase function needs to be checked; (2) ART model is designed for medium with weakly absorption properties, thus it cannot be used for certain SGS and SPS, especially for long wavelength (e.g. 1.6 μm). In short, we cannot really avoid making certain (explicit or hidden) assumptions of SPS if it is not iteratively retrieved in the algorithm, like in the eXtensible Bremen Aerosol/cloud and surfacE parameters Retrieval (XBAER) algorithm.

- **Highlighting with respect to the XBAER retrieved SPS**: We believe our work, as a first step/attempt, provides some new/useful way/information for the SPS. However, we should not over-interpret the shape we retrieved.

This paper is structured as follows: instrument characteristics of SLSTR and the field-based measurements ~~*in-situ*~~ and aircraft measurements used for validation are described in section 2. Section 3 describes the method including cloud screening, atmospheric correction, and the flowchart of the ~~eXtensible Bremen Aerosol/cloud and surfacE parameters Retrieval (~~XBAER~~)~~ algorithm. Some selected data products and comparisons with MODIS products and field-based measurements~~*in situ* data~~ are shown in section 4. The comparison with the recent campaign measurement is presented in section 5. A discussion to ~~show~~ illustrate a time series of the retrieval results is shown in section 6. The conclusions are given in section 7.

2 Data

2.1 SLSTR instrument

After the loss of Environmental Satellite (Envisat) on 12 April 2012, the European Space Agency (ESA) launched Sentinel-3A, Sentinel-3B in February 2016, and April 2018, respectively. As the successor of Advanced Along-Track Scanning Radiometer (AATSR) onboard Envisat, Sentinel satellites take the SLSTR instrument. The SLSTR instrument has similar characteristics as compared to AATSR (see Table 1 for details). The instrument has nine spectral bands in the visible and infrared spectral range. It also has dual-view observation capability with swath widths of 1420 km and 750 km for nadir and oblique directions, respectively. The SLSTR and ~~/~~AATSR dual-view observations of the Earth's surface make surface Bidirectional Reflectance Distribution Function (BRDF) effect estimation possible, which is widely used to retrieve both surface and atmospheric geophysical parameters (Popp et al., 2016). Besides the heritage of AATSR, some new features (wider swath, new spectral bands and higher spectral resolution for certain bands) have been included in SLSTR instrument (https://sentinel.esa.int/web/sentinel/technical-guides/sentinel-3-slstr/instrument).

Table 1 Instrument characteristics of AATSR and SLSTR

SLSTR			AATSR		
Band #	**Central wavelength(μm)**	**Resolution(m)**	**Band #**	**Central wavelength(μm)**	**Resolution(m)**
1	0.555	500	4	0.555	1000
2	0.659	500	5	0.659	1000
3	0.865	500	6	0.865	1000
4	1.375	500			
5	1.610	500	7	1.610	1000

6	2.25	500			
7	3.74	1000	1	3.74	1000
8	10.85	1000	2	10.85	1000
9	12	1000	3	12	1000
10	3.74	1000			
11	10.85	1000			

2.2 Ground-based measurements

The validation of satellite derived snow properties is challenging due to i) limited available field-based measurements; ii) the difficulties of spatial-temporal collocation between satellite observations and field-based measurements because of cloud coverage. This manuscript focuses on the Sentinel-3a satellite for the period of February 2016 (lauch month of Sentinel-3a) and December 2020. The field-based measurements from both permanent sites and campaign sites for the focusing time period are collected. Fig. 1 shows the geographic distribution of the validation sites. The site names used in this manuscript are listed near each site. Since XBAER retrieves SGS, SPS and SSA simultaneously, the SnowEx campaign, which provides three parameters as well, will be introduced detailed first.

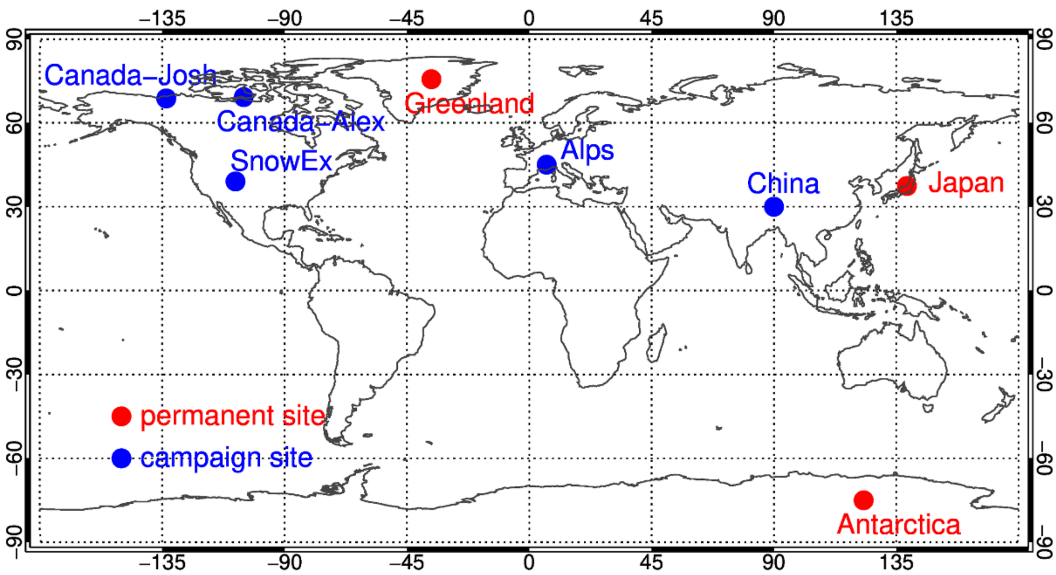

Fig. 1 Geographic distribution of the validation sites. The colors represent the type of each site while the site name used in this manuscript is indicated near each site.

NASA established a terrestrial hydrology program (SnowEx mission) in order to better quantify the amount of water stored in snow-covered regions (Kim et al., 2017). The measurements for the first year (2016 - 2017) were carried out during February 2017 (between 08 February 2017 and 25 February 2017) at Grand Mesa and the Senator Beck Basin in Colorado (hereafter refer as SnowEx17) (See Fig. ~~1~~ 2 (~~b~~a)) (Elder et al., 2018). Grand Mesa is a forest region covered by relatively homogeneous snow cover with an area size similar to airborne instrument swath widths (Brucker et al., 2017) (See Fig. ~~1~~ 2 (~~a~~c)). Senator Beck Basin site has a complex topography and covered by snow. The campaign used more than 30 remote sensing instruments and most of the instruments are from the National Aeronautics and Space Administration (NASA) except some instruments such as the ~~European Space Agency,~~ ESA's Radar (Kim et al., 2017). The snowpits measurements provide information of snow grain size and type/shape, stratigraphy profiles, and temperatures with certain information about surface conditions (e.g. snow roughness) (Rutter et al., 2018). The SnowEx17 campaign provides seven different shapes (New Snow, Rounds, Facets, Mixed Forms, Melt-Freeze, Crust, and Ice Lens). Table 2 lists both the SnowEx17 measured snow grain shapes and SPSs defined in Yang et al. (2013). The SPSs defined by ICSSG are also listed in the table and the possible linkage between Yang SPS and ICSSG SPS (named as SPS similarity) will be discussed later.~~An example of the snow structure/roughness can be seen from Fig. 1 (c).~~ The measurements have been publicly released in nsidc.org/data/snowex. The data was collectd in SnowEx20 for the period of 27 January and 12 February, 2020.

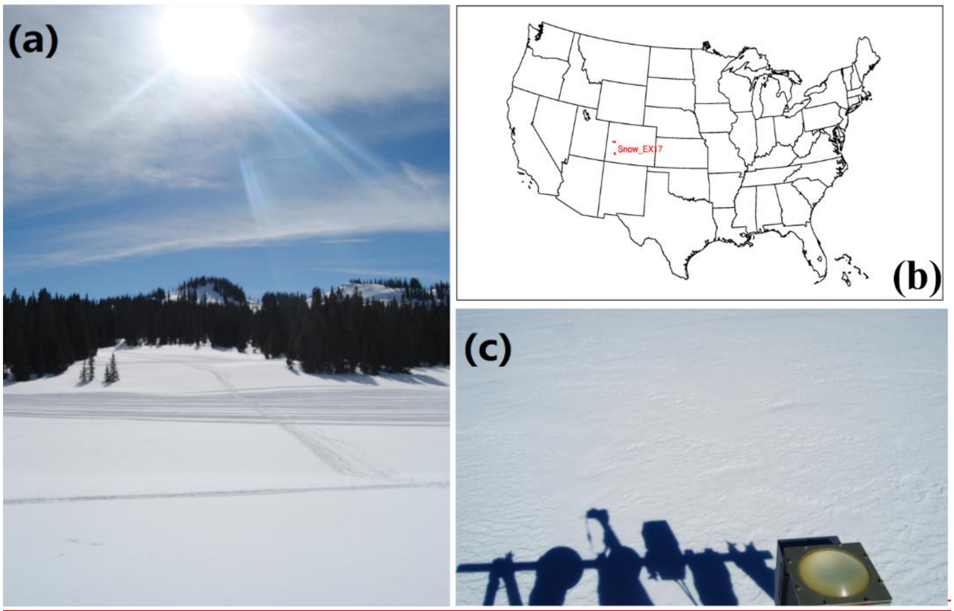

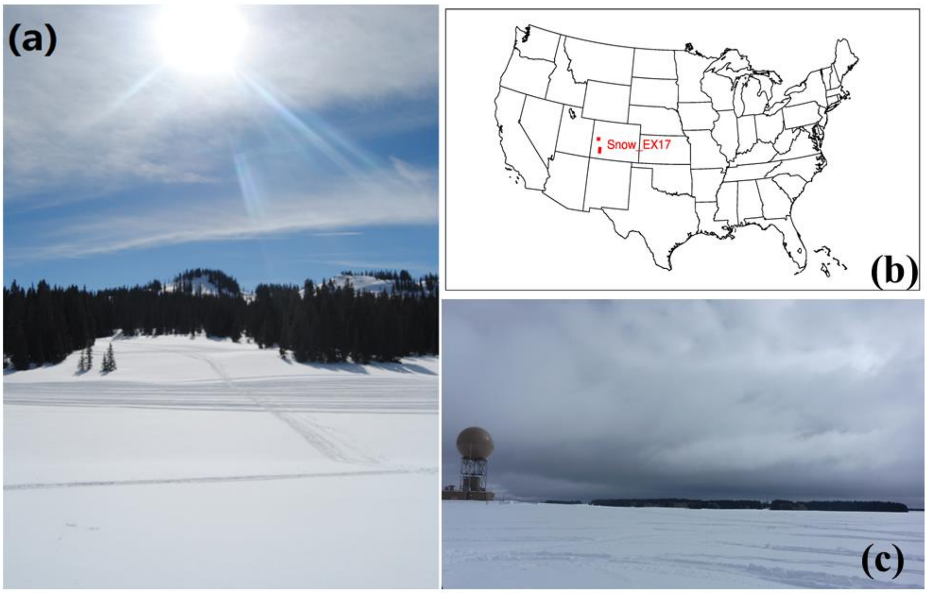

Fig. ~~1~~ 2 Photos taken during the SnowEx~~17~~ campaign. (a) An overview of the campaign environment around Senator Beck Basin site; (b) Location of SnowEx~~17~~ campaign (red rectangles); (a) An overview of the campaign environment around Grand Mesa site;~~(c) A detailed example of measured snow structure/roughness (Image/photo courtesy of A~~. Roy, A. Langlois, and L. Brucker; supplied by the National Snow and Ice Data Center, University of Colorado, Boulder~~.~~)

The measurements over Greenalnd are obtained by the EastGRIP team over (75.63°N,36.004°W) . Detailed information of the site can be found at https://eastgrip.org.

The data have been used to validate the SGS and SSA derived from OLCI (Kokhanvosky et al., 2018). The same dataset, covering the period of May 2017 and August 2018 is used in this manuscript.

The SSA measurements at Nunavut, Northern Canana (69.20°N,104.80°W) were obtained using the instrument described by Montpetit et al. (2012). The observation period covers April, 2018. SGS or SSA is calculated using the relationship between SSA and SGS if SSA or SGS is not measured.

The SPS and SSA measurements around Inuvik, Northwest Territories of Canana (68.73°N,133.49°W) covers the period of November 2018 – March 2019. There were three deployments, the freeze-up period (November 2018), the strom input period (Janauray 2019) and the metamorphosis period (March 2019) (King et al., 2019).

The SSA measurements above Frech Alps (45.04°N,6.41°W) were collected in the snow seasons during 2016 – 2018 (Tuzet et al,, 2020). The measurements for 2016 – 2017 period provide SSA profile information with vertical resolution of 3 cm using the DUFISSS instrument (Gallet et al., 2009). For the period of 2017 -2018, the measurements were obtained with vertical resolution of 6 cm using the Alpine Snowpack Specific Surface Area Profiler (Libois et al., 2014). The uncertainty is estimated to be 10%.

The SGS measuremnts were obtained over Nagaoka, Japan (37.41°N,138.88°W) (Yamaguchi et al., 2019; Avanzi et al., 2019). The observations during January, 2017 – March 2018 are used in this manuscript.

The SGS measurements were obtained over Xingjiang province during diferent period (Chen et al., 2020), the dataset around the site (44.146°N,85.848°E) for the period November 2018 – November 2019 is used in this manuscrip.

The SSA measurements at Dome C (75°S,123°E) in Antarctica cover the period of 2016 – 2018, the accracy of the measurments is better than 15% (Picard et al., 2016). The data were collected using a self-designed and assembled insturment, named as Autosolexs, which can be used to measure the snow properties for several years under the harsh environment.

Table 2 Snow grain type (shape) provided by Yang et al (2013) ~~and~~ , *in-situ* measurements in SnowEx campaign and by ICSSG. Please note here the grain type ~~in~~ by Yang et al. ~~and~~ ,measured in SnowEx~~17~~ and provided by ICSSG given in the same line have no 1:1~~not~~ linkage

~~Yang~~			~~SnowEx17~~
~~Grain Type~~	~~Abbriation~~	~~Schematic drawing~~	~~Grain Type~~
~~Aggregate of 8 columns~~	~~col8e~~		~~New Snow~~
~~Droxtal~~	~~droxa~~	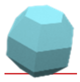	~~Rounds~~
~~Hollow bullet rosettes~~	~~holbr~~		~~Facets~~
~~Hollow column ,~~	~~holco~~	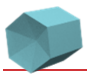	~~Mixed Forms~~
~~Plate~~	~~pla_1~~	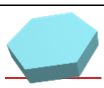	~~Melt-Freeze~~
~~Aggregate of 5 plates~~	~~pla_5~~	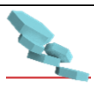	~~Crust~~
~~Aggregate of 10 plates~~	~~pla_10~~		~~Ice Lens~~
~~Solid bullet rosettes~~	~~solbr~~	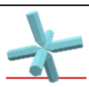	-
~~Column~~	~~soleo~~		-

Yang			SnowEx	ICSSG	
Grain Type	Abbriation	Schematic drawing	Grain Type	Grain Type	Abbriation
Aggregate of 8 columns	col8e		New Snow	Precipitation Particles	PP
Droxtal	droxa	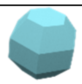	Rounds	Machine Made snow	MM
Hollow bullet rosettes	holbr		Facets	Decomposing and Fragmented	DF
Hollow column ,	holco	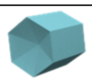	Mixed Forms	Rounded Grains	RG
Plate	pla_1	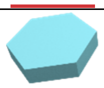	Melt-Freeze	Faceted Crystals	FC

Aggregate of 5 plates	pla_5		Crust	Depth Hoar	DH
Aggregate of 10 plates	pla_10		Ice Lens	Surface Hoar	SH
Solid bullet rosettes	solbr		-	Melt Forms	MF
Column	solco		-	Ice Formations	IF

2.3 Aircraft observations

During the Polar Airborne Measurements and Arctic Regional Climate Model Simulation Project (PAMARCMiP) campaign held in March/April 2018 ground-based and airborne observations of surface, cloud and aerosol properties were performed near the Villum Research Station (North Greenland). One of the most important objectives of the PAMARCMiP 2018 campaign ~~is~~ was to quantify the physical and optical properties of snow, sea ice and atmosphere (Egerer, et al., 2019; Nakoudi et al., 2020). Airborne spectral irradiance measurements by the Spectral Modular Airborne Radiation Measurement System (SMART) onboard the Polar 5 research aircraft operated by Alfred-Wegener-Institut were used to derive snow grain sizes along the flight track. The SMART provides solar up- and downward spectral irradiances in the range between 0.4 – 2.0 µm. The optical inlets are actively horizontally stabilized with respect to aircraft movement (Wendisch et al., 2001) within 5° pitch and roll angle. In particular, for high solar zenith angles (SZA) as presented during PAMARCMiP (about 80° SZA), misalignment of the optical inlets implies significant measurement uncertainties (Wendisch et al., 2001). Further uncertainties are related to the spectral and radiometric calibration, as well as the correction of the cosine response which sums up to a total wavelength-dependent uncertainty (one sigma) for the irradiances ranging between 3 to 14% (Jäkel et al., 2015). The derivation of the surface albedo from aircraft observations requires atmospheric corrections due to the atmospheric attenuation and scattering by gases and aerosols~~masking by gases and molecules~~. There an iterative method to correct for these effects was applied according to the procedure described by Wendisch et al. (2004). The retrieval of the snow grain sizes is based on the method described in Carlsen et al. (2017) which uses a modified approach presented by Zege et al. (2011).

3 Methodology

3.1 Cloud screening

The algorithm synergistically uses SLSTR and OLCI data to identify clouds over the snow surface. The criteria for cloud screening over snow using SLSTR and OLCI measurements can be found in Istomina et al. (2010) and Mei et al. (2017), respectively. Short summaries of Istomina et al. (2010) and Mei et al. (2017) are presented below and more details can be found in the original publications. The algorithm proposed by Istomina et al. (2010) for the SLSTR instrument utilizes spectral behavior differences at SLSTR visible and thermal infrared channels, and this algorithm is updated later by Jafariserajehlou et al. (2019). Relative thresholds ~~have~~ are determined based on radiative transfer simulations under various atmospheric and surface conditions. The method proposed by Mei et al. (2017) for the OLCI instrument uses different cloud characteristics: cloud brightness, cloud height, and cloud homogeneity. The TOA reflectance at 0.412 µm, the ratio of TOA reflectance at 0.76 and 0.753 µm, standard deviation of TOA reflectance at 0.412 µm are used to characterize cloud brightness, cloud height, and cloud homogeneity, respectively. A pixel is identified as a cloud-free snow pixel when both SLSTR and OLCI identify it as a cloud-free snow pixel. Identified clouds can be surrounded by a so-called "twilight zone" (Koren et al., 2007), which can extend more than ten kilometers from a cloud pixel to a cloud-free area. The surrounding 5×5 pixels of an identified cloud pixel will be marked as a cloud to avoid the "twilight zone" effect. A more ~~details~~ detailed description of this cloud screening method can be found in Mei et al. (2020a). Addtionally, TOA reflectance at 0.55 µm is required to be higher than 0.5 to avoid dark ice and dirty snow.

3.2 Atmospheric correction

Due to the low atmospheric aerosol loading over the Arctic snow covered regions (e.g. Greenland), atmospheric correction using path radiance representation (Chandrasekhar, 1950; Kaufman et al., 1997) can provide accurate estimation of surface reflection even under relatively large SZA (Lyapustin, 1999). The TOA reflectance at selected channels (0.55 and 1.6 μm) is described by the path radiance representation (Chandrasekhar, 1950; Kaufman et al., 1997) as:

$$R(\theta,\theta_0,\varphi,\tau,AT) = R^0(\theta,\theta_0,\varphi,\tau,AT) + \frac{T(\theta,\theta_0,\tau,AT)A}{1-s(\tau,AT)A}, \quad (1)$$

where $R^0(\theta,\theta_0,\varphi,\tau,AT)$ is the TOA reflectance calculated assuming black surface (surface reflectance equal 0) under VZA, SZA and RAA of θ,θ_0,φ. τ and AT are AOT and aerosol type. $T(\theta,\theta_0,\tau,AT)$ is the total (diffuse and direct) transmittance from the sun to the surface and from surface to the satellite, $s(\tau,AT)$ is spherical albedo, A is Lambertian surface albedo. The spherical albedo is the fraction of the incident solar radiation diffusely reflected over all directions (albedo of an entire planet). The Lambertian surface albedo is defined as the ratio of reflected to incident flux. The atmospheric correction is performed based on the following equation:

$$A = \frac{R(\theta,\theta_0,\varphi,\tau,AT) - R^0(\theta,\theta_0,\varphi,\tau,AT)}{(R(\theta,\theta_0,\varphi,\tau,AT) - R^0(\theta,\theta_0,\varphi,\tau,AT))s(\tau,AT) + T(\theta,\theta_0,\tau,AT)}. \quad (2)$$

The atmospheric correction is based on the Look-Up-Table (LUT) precalculated using radiative transfer code SCIATRAN (Rozanov et al., 2014). The radiative transfer calculations were performed assuming AOT values provided by MERRA simulations and aerosol type defined as weakly absorbing according to ~~our~~ a previous investigation (Mei et al., 2020b).

3.3 XBAER Algorithm

The theoretical background of the retrieval algorithm is given in section 4 of the companion paper. The XBAER algorithm consists of three stages to derive SGS, SPS, and SSA: 1) derivation of SGSs for each predefined SPS; 2) selection of the optimal SGS and SPS pairs for each scenario; 3) calculation of SSA for each retrieved SGS and SPS. This section describes some implementation details such as the selection of the first guess for the retrieval parameters and the flowchart of the algorithm.

A reasonable first guess value for the iteration process can significantly reduce the computation time, which is important for retrievals of atmospheric and surface properties over large geographic and temporal scales with different instrument spatial resolutions. The first guess of SGS in the XBAER algorithm is obtained employing the semi-analytical snow reflectance model (Kokhanovsky and Zege, 2004; Kokhanovsky et al., 2018). Details of using this model to derive SGS can be found in Lyapustin et al. (2009). Due to the different band settings in MODIS and SLSTR (SLSTR has no 2.1 µm channel as MODIS), one non-absorption channel (0.55 µm) and one absorption channel (1.6 µm) are used in our SLSTR retrieval algorithm.

Fig. ~~2~~ 3 shows the flowchart of how XBEAR derives SGS, SPS, and SSA. The flowchart includes pre-processing of cloud screening using the synergy of OLCI and SLSTR and the atmospheric correction using MERRA providing AOT and weakly absorbing aerosol type. The SGS and SPS are obtained using the LUT-based minimization routine. SSA is then calculated using the retrieved SGS and SPS.

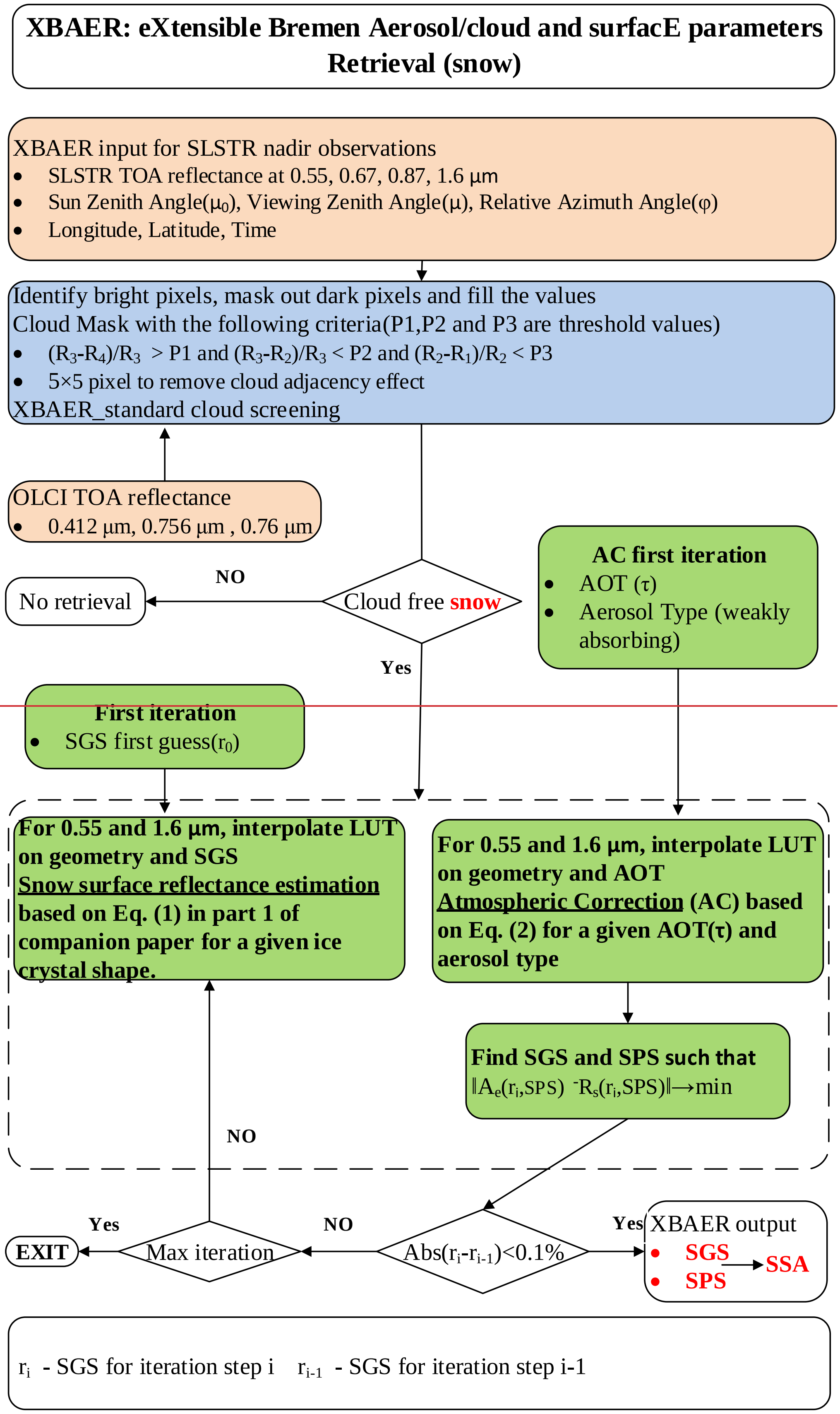
XBAER: eXtensible Bremen Aerosol/cloud and surfacE parameters Retrieval (snow)
XBAER input for SLSTR nadir observations
SLSTR TOA reflectance at 0.55, 0.67, 0.87, 1.6 µm
Sun Zenith Angle(µ0), Viewing Zenith Angle(µ), Relative Azimuth Angle(φ)
Longitude, Latitude, Time
Identify bright pixels, mask out dark pixels and fill the values
Cloud Mask with the following criteria(P1,P2 and P3 are threshold values)
(R3-R4)/R3 > P1 and (R3-R2)/R3 < P2 and (R2-R1)/R2 < P3
5×5 pixel to remove cloud adjacency effect
XBAER_standard cloud screening
OLCI TOA reflectance
0.412 µm, 0.756 µm , 0.76 µm
No retrieval
NO
Cloud free snow
Yes
AC first iteration
AOT (τ)
Aerosol Type (weakly absorbing)
First iteration
SGS first guess(r0)
For 0.55 and 1.6 µm, interpolate LUT on geometry and SGS
Snow surface reflectance estimation based on Eq. (1) in part 1 of companion paper for a given ice crystal shape.
For 0.55 and 1.6 µm, interpolate LUT on geometry and AOT
Atmospheric Correction (AC) based on Eq. (2) for a given AOT(τ) and aerosol type
Find SGS and SPS such that
‖Ae(ri,SPS) -Rs(ri,SPS)‖→min
NO
Yes
EXIT
Max iteration
NO
Abs(ri-ri-1)<0.1%
Yes
XBAER output
SGS
SPS
SSA
ri - SGS for iteration step i   ri-1 - SGS for iteration step i-1

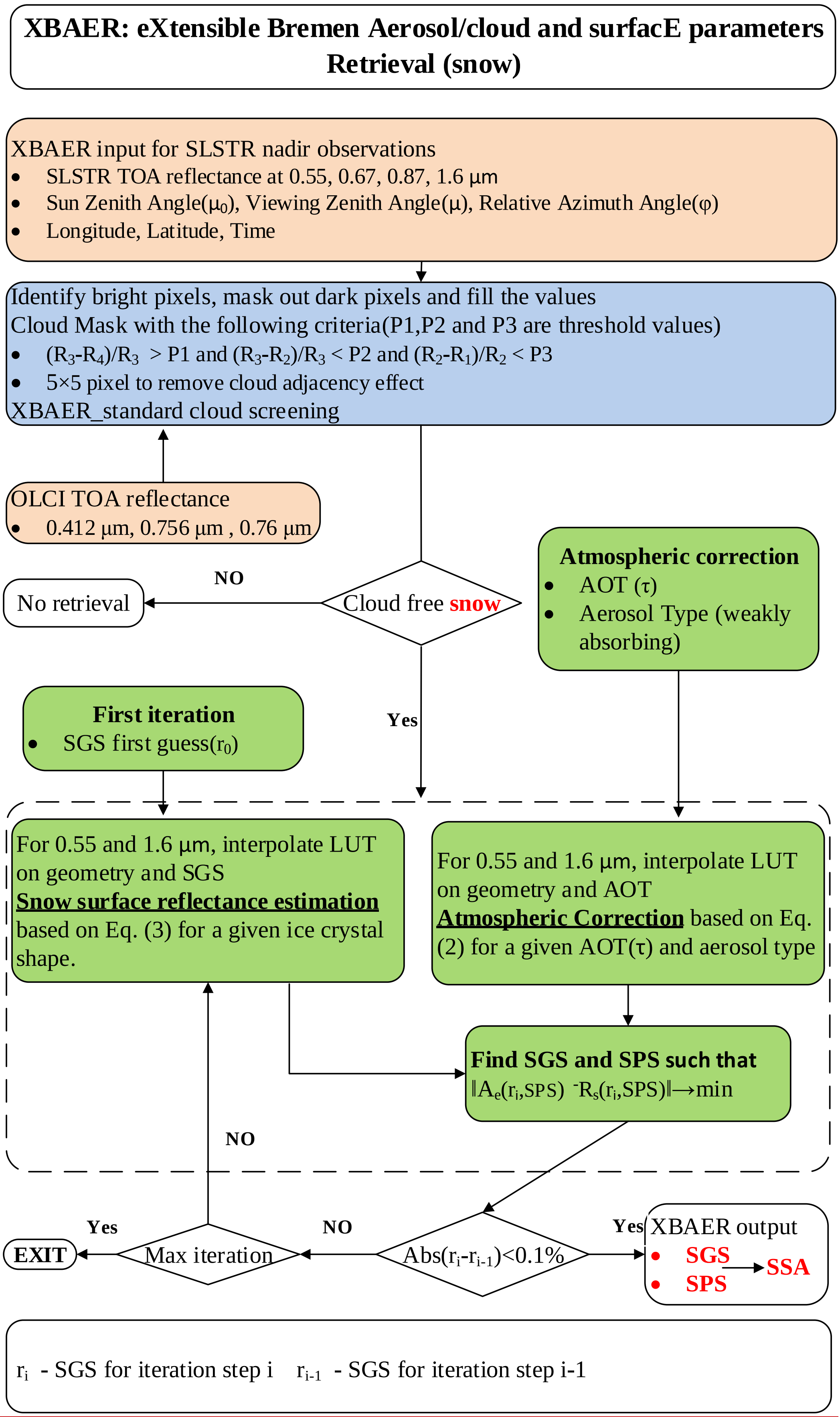
XBAER: eXtensible Bremen Aerosol/cloud and surfacE parameters Retrieval (snow)
XBAER input for SLSTR nadir observations
SLSTR TOA reflectance at 0.55, 0.67, 0.87, 1.6 μm
Sun Zenith Angle(μ0), Viewing Zenith Angle(μ), Relative Azimuth Angle(φ)
Longitude, Latitude, Time
Identify bright pixels, mask out dark pixels and fill the values
Cloud Mask with the following criteria(P1,P2 and P3 are threshold values)
(R3-R4)/R3 > P1 and (R3-R2)/R3 < P2 and (R2-R1)/R2 < P3
5×5 pixel to remove cloud adjacency effect
XBAER_standard cloud screening
OLCI TOA reflectance
0.412 μm, 0.756 μm , 0.76 μm
NO
No retrieval
Cloud free snow
Atmospheric correction
AOT (τ)
Aerosol Type (weakly absorbing)
First iteration
SGS first guess(r0)
Yes
For 0.55 and 1.6 μm, interpolate LUT on geometry and SGS
Snow surface reflectance estimation based on Eq. (3) for a given ice crystal shape.
For 0.55 and 1.6 μm, interpolate LUT on geometry and AOT
Atmospheric Correction based on Eq. (2) for a given AOT(τ) and aerosol type
Find SGS and SPS such that
‖Ae(ri,SPS) -Rs(ri,SPS)‖→min
NO
Yes
EXIT
Max iteration
NO
Abs(ri-ri-1)<0.1%
Yes
XBAER output
SGS
SPS
SSA
ri - SGS for iteration step i ri-1 - SGS for iteration step i-1

Fig. ~~2~~ 3 Flow chart of the XBAER retrieval algorithm

4 Results and Comparison

Greenland is the largest ice-covered land mass in the northern hemisphere and the biggest cryospheric contributor to the global sea-level rise (Ryan et al., 2019). XBAER derived SGS, SPS, and SSA over Greenland enable a good understanding of the retrieval accuracy with a large and representative geographic scale. Kokhanovsky et al., (2019) reported that July is an optimal month to analyze satellite-derived snow properties over Greenland because Greenland has a strong Snow Particle Metamorphism Process (SPMP) due to higher temperatures in July (Nakamura et al. 2001). The SPMP, affected strongly by temperature, is a dominant factor for the variabilities of SGS, SPS, and SSA (LaChapelle,1969; Sokratov and Kazakov, 2012; Saito et al., 2019). Snow particle size increases dramatically and the ice crystal particles are compacted in the strong SPMP (Aoki et al., 1999; Nakamura et al. 2001; Ishimoto et al. 2018).

Fig. ~~3~~ 4 shows an example of the XBAER-derived SGS on 28 July 2017 from SLSTR, XBAER first guess and its comparison with the same scenario from MODSCAG product (Painter et al., 2009). Here we chose MODIS/Aqua rather than MODIS/Terra to avoid the impact of instrument degradation of MODIS/Terra (Lyapustin et al., 2014). The visualization of XBAER-derived SGS is shown to be between 10 and 500 μm. The XBAER first guess has in general low value (Lyapustin et al., 2009), as compared to XBAER and MODSCAG results, . The XBAER and MODSCAG derived SGS show good agreement on the geographic distribution. The slight difference of cloud covered regions (white parts) is explained by the different overpass time between SLSTR and MODIS. Both algorithms demonstrate that SGSs in central Greenland are smaller than those at coastline regions. This is attributed to the geographic distribution of surface temperature over Greenland. In particular, central Greenland has a significantly higher elevation and the impacts of imperfect atmospheric correction on retrieved snow properties are ignorable. The lower temperature under higher elevation regions has weaker SPMP, producing more irregular SPS. The situation is opposite in the coastline regions over Greenland. Since Fig. 4 is composited by three different SLSTR orbits, the geometrical-shaped features in Eastern Greenland are caused by the effective Lambertian albedo assumption in XBAER algorithm. This assumption introduces addtional bias under large viewing zenith angle condition, which occurs at the edge of each SLSTR orbit.

Fig. 4 5 shows XBAER retrieved SGS, SPS, and SSA for 28 July 2017. Since there are no available products of SPS and SSA from MODSCAG, it is a great challenge to do a similar comparison as in the case of SGS. Fortunately, campaign-based and laboratory investigations provide valuable information on typical snow shapes under different times/locations with a wide range of atmospheric conditions (humidity, temperature, ... etc.). Kikuchi et al. (2013) proposed a global classification of snow particle shape based on 21 snow/ice crystal observation sites. According to Kikuchi et al. (2013), the typical SPSs in the polar regions include column crystal (e.g. solid column, bullet-type crystal) with SGS of about 50 μm for solid column and between 100 μm and 500 μm for bullet-type, the germ of ice crystal group with SGS of less than 50 μm. Saito et al. (2019) pointed out that SPSs of fresh snow in the polar regions are typically a mixture of irregular shapes such as column and platelike shape. Ishimoto et al. (2018) found that aged snow can have an aggregate structure. The optical properties of small ice crystal particles in aged snow may be well-characterized by granular/roundish shapes, while SPS tends to be irregular or severely roughened shapes during the SPMP (Ishimoto et al., 2018). Pirazzini et al (2015) investigated the impact of ice crystal sphericity on the estimation of snow albedo and found droxtal is a reasonable assumption to take ice particle non-sphericity into account. The above conclusions can be used as „qualitative reference“ to understand the satellite-derived SPS. In the meantime, a large proportion of ice-sheet melts during the warm July, which unequivocally leads to rounded coarse grains very quickly. According to Fig. 45, central Greenland is largely covered by small particles with roundish/droxtal shape while coastline regions are covered to be aggregated shapes (aggregate of 8 columns, aggregate of 5 plates, the aggregate of 10 plates) with large particle sizes, are essentially attributed to the different SPMP over different regions of Greenland. Bullet-type crystal (solid bullet rosettes) occurred with SGS of about 100 μm. The examples shown in Fig. 4 5 can be reasonably explained by previous publications (Kikuchi et al., 2013; Pirazzini et al., 2015; Ishimoto et al.,2018; Saito et al., 2019).

The geographic distribution of SSA is somehow anti-correlated with the geographic distribution of SGS, due to the definition of SSA. Most SSA fall into the range of 10-40 m^2/kg, which agrees with previous publication (Kokhanovsk et al., 2019). The change of SSA occurs especially after snowfall (Carlsen et al., 2017; Xiong et al., 2018). Since SSA contains both information of SGS and SPS and field measurements provide SSA, the validation of SSA can be also used as an „indirect quantitative validation“ of SPS, which will be quantitatively presented in the next section.

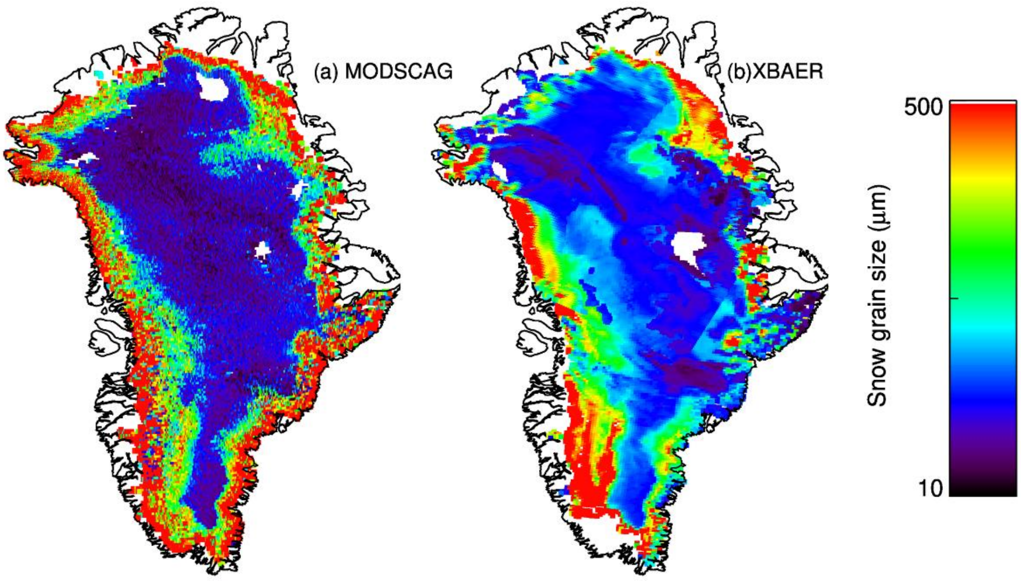

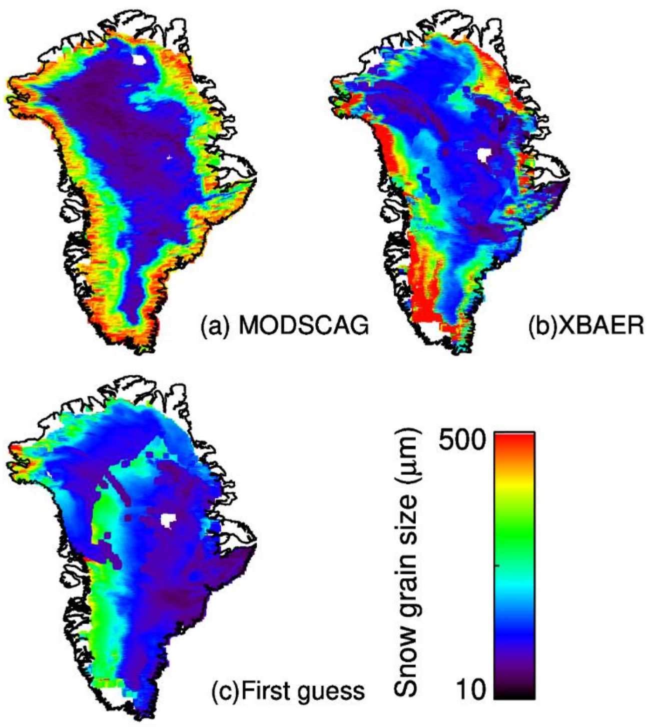

Fig ~~3~~4. A comparison of the MODISSCAG ~~snow grain size~~SGS (a) ~~and~~ ; XBAER derived ~~snow grain size~~SGS (b) and first guess (c) over Greenland on 28 July, 2017.

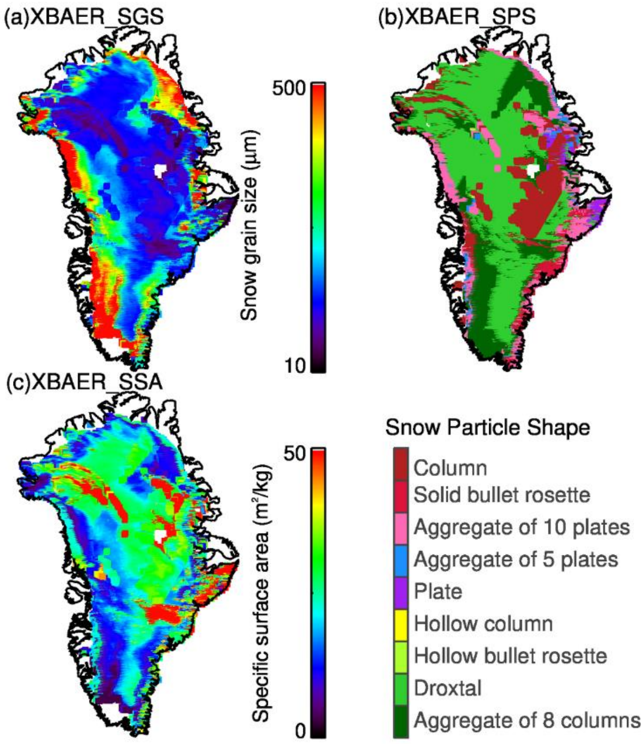

Fig ~~4~~5. XBAER derived ~~snow grain size~~SGS, SPS and SSA~~snow grain shape~~ over Greenland for the same scenario as in Fig. ~~3~~4.

5 ~~Comparison and~~ Validation

In this section, we will quantitatively ~~compare/~~validate XBAER derived snow properties with ~~ground~~field-based and ~~/~~aircraft measurements. ~~We emphasize that the results presented in this section is considered as preliminary and the validation of our satellite-derived snow products will be complemented by the MOSAiC expedition, which is now ongoing.~~

5.1 ~~Comparison~~ Validation ~~with the~~using the observations of SnowEx17 campaign

~~The above analysis shows that the XBAER is capable to derive SGS, SPS, and SSA, which agrees reasonably well with existing satellite products or can be qualitatively explained by campaign-based and laboratory findings.~~ In order to have a quantitative evaluation of XBAER-derived SGS, SPS, and SSA, we have collocated the SLSTR observations with recent campaign measurements provided by SnowEx17 and SnowEx20, as described in section 2. Due to overpass time and cloud cover, only limited match-ups between XBAER retrievals and SnowEx17 and SnowEx20 measurements have been obtained. No match-up is obtained for SnowEx20.

Table 3 summarizes match-up information. The first three columns in Table 3 show the observation times and locations (longitude and latitude). The fourth and fifth columns indicate the cloud conditions. Cloud conditions in Table 3 are given by three categories: cloud-free snow, cloud-contaminated snow, and cloud-covered snow. These three categories are classified by the XBAER cloud identification results (see Section 3.1) and are illustrated by the RGB composition figures, covering the SnowEx campaign area, as presented in Fig. 46. An optically thin cloud over a melting snow layer, a thick cloud over snow, and snow scenarios are presented in Fig. 4 6 (a), (b) and (c), respectively. The cloud optical thickness (COT), estimated using the independent XBAER cloud retrieval algorithm, as presented in Mei et al (2018), is ~0.5 and ~10 for 9th and 11th February, respectively.

Table 3 Information of Match-ups between SnowEx and SLSTR during February, 2017

Date	Lon(°)	Lat(°)	COT	Comment
02-09	-108.1092	39.0369	~0.5	cloud-contaminated snow
02-22	-108.0634	39.0444	0	cloud-free snow
02-22	-108.0625	39.0459	0	cloud-free snow
02-22	-108.0617	39.047	0	cloud-free snow
02-11	-108.0462	39.0278	~10	cloud-covered snow

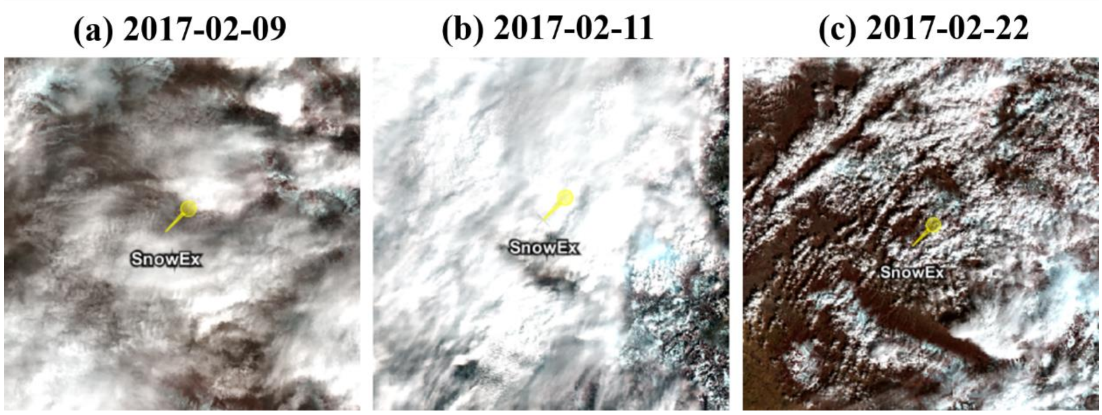

Fig ~~4~~6. Zoom-in of the RGB composition figures (created using ESA official SLSTR software SNAP) for the selected 3 days presented in Table 3. The yellow point indicate the SnowEx instrument position.

Even though the synergistical use of SLSTR and OLCI provides valuable information to separate cloud and snow, the identification of an optically thin cloud above a snow layer is a great challenge due to the similar wavelength dependence of snow and cloud reflectance, especially between snow and ice cloud (Mei et al., 2020). The identification of the cloud from an underlying snow layer in XBAER relies mainly on the O_2 channel on OLCI instrument, which provides the cloud height information (Mei et al., 2017). Fig. ~~5~~ 7 shows the performance of XBAER cloud identification results for cloud contamination and cloud-covered snow scenarios. The red star indicates the measurement location. The zoom-in figures around the measurement site ~~is~~ are presented in Fig. ~~4~~ 6 above. XBAER cloud screening shows, in general, a good performance according to the RGB visual interpretation. However, part of the thin cirrus cloud on the 9th of February is not correctly avoided. For 9th of February, XBAER cloud identification gives a result of clean snow while it contains a thin cloud above a snow layer. For the 11th of February, XBAER has successfully detected the cloud from an underlaying snow layer. For a comprehensive investigation of XBAER derived snow properties under all snow-cloud coupled conditions, the ~~fifth~~ match-up on 11th February 2017 (labeled as grey) has been manually set to be „cloud free snow“. The reason to perform the validation for different cloud conditions is that the satellite retrieval can only be performed under cloud-free conditions while field measurements may be obtained under cloud conditions, especially when fresh snow properties are measured. Thus, the field-based measurements under full-cloud or partly-cloudy conditions are still valuable in the validation process (Jeoung et al., 2020). According to the sensitivity study, cloud contamination leads to an underestimation of SGS and the overestimation of SSA, depending on the cloud fraction.

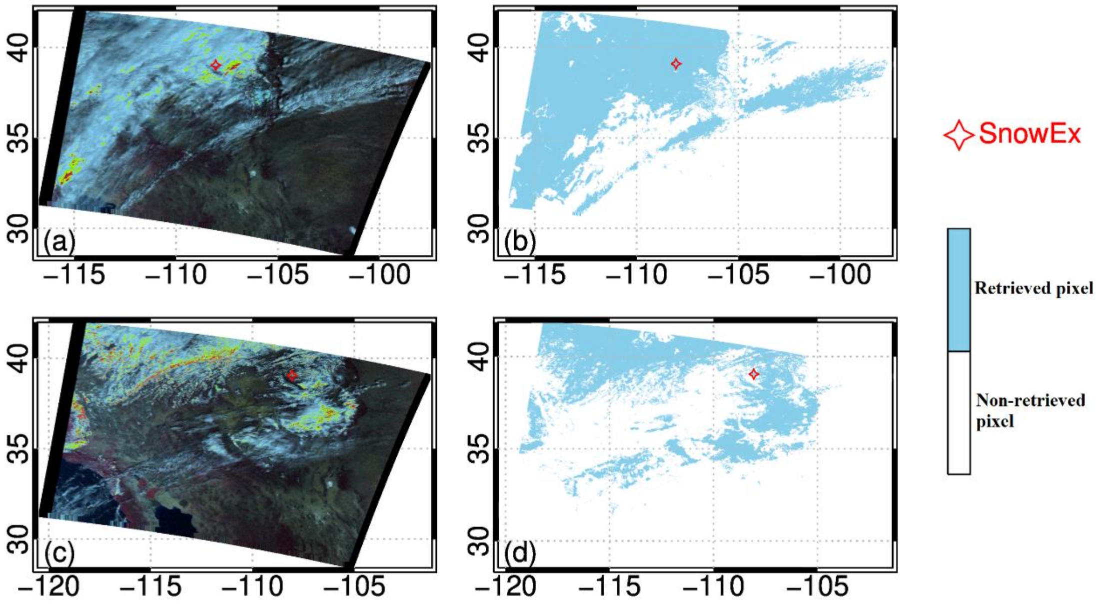

Fig ~~5~~7. The RGB composition (left column) for 9 (a) and 22 (c) February when XBAER detect as cloud free snow and provides the retrieval. The XBAER cloud screening results (right column) for the corresponding days are given in (b) and (d). The "Retrieved pixel" legend refers to cloud free snow. The "Non-retrieved pixel" legend refers to the area where XBAER retrieval is not performed, this includes (1) snow-free and cloud free (2) cloud above snow; (3) cloud above snow-free.

Table 4 summarizes the comparison between XBAER retrieval results, MODSCAG product, and SnowEx17 campaign measurements. The first three columns in Table 4 are the same as Table 3, showing the observation time and locations (longitude and latitude). The second three columns are the SnowEx17 measured SGS. Since the SnowEx17 provides the SGS profile up to 1 meter depth, the minimum (SnowEx_min), average (SnowEx_avg), and maximum (SnowEx_max) values of SGS are listed in Table 3. The last two columns are MODSCAG and~~is~~ XBAER derived SGS. For the four cloud-filter-passed match-ups, XBAER-derived SGS shows good agreement with SnowEx17 measurements, especially for the 22nd of February. The average absolute difference is less than 10 μm (4 % in relative difference). The relatively large SGS (⩾ 250μm) caused mainly by the warm-up on the 21st of February (see the comment in Table 5, reported by campaign participators), ~~the warmer condition~~which leads to a quicker snow metamorphism process, forming large ice crystal particles. MODSCAG only provides retrieval results for 9th and 11th Feb. The results from XBAER and the MODSCAG agree well. This possibly indicate a similar performance between XBAER and the MODSCAG.

An underestimation is found for the first match-up on the 9th of February. This is explained by the cirrus cloud contamination as presented in Fig. ~~4 and 5~~11. According to ~~our~~ an independent XBAER cloud retrieval (Mei et al., 2018), the COT is ~0.5, cloud contamination with COT=0.5 introduces ~30% underestimation according to ~~Fig~~fig. 11 in part 1 of the companion paper. So for SGS=100 µm, provided by SnowEx, XBAER is expected to have a theoretically retrieved SGS of ~ 70 µm while a value of 78.2 µm is obtained from the real satellite retrieval. In order to further confirm this negative bias feature caused by cloud contamination, 11th February (a snowstorm at the measurement site is reported by campaign participators), although filtered by the XBAER cloud screening routine, is forced to retrieve the full-cloud-covered scenario as a cloud-free case. According to the theoretical investigations presented in part 1 of the companion paper, for COT⩾5, the XBAER algorithm retrieves cloud effective radius, rather than SGS. The retrieved ice crystal size depends on the cloud effective radius of the cloud above the underlying snow layer. The independent XBAER cloud retrieval provides SGS value of ~ 38 µm while 32.3 µm is obtained by the XBAER snow retrieval, for a reference value of 100 µm as provided by SnowEx17 measurement. This is consistent with a typical ice cloud effective radius (King et al., 2013; Mei et al., 2018), under a snowstorm condition.

Table 4 The comparison between SnowEx SGS measurements,~~and~~ XBAER and MODSCAG retrieved SGS during February, 2017.

Date	Lon(°)	Lat(°)	SnowEx_min(µm)	SnowEx_avg(µm)	SnowEx_max(µm)	MODSCAG (µm)	XBAER(µm)
02-09	-108.1092	39.0369	50	100	150	90	78.2
02-11	-108.0462	39.0278	50	100	200	40	32.3
02-22	-108.0634	39.0444	100	250	500	-	254.4
02-22	-108.0625	39.0459	150	250	400	-	254.4
02-22	-108.0617	39.047	100	200	300	-	215.7
~~02-11~~	~~-108.0462~~	~~39.0278~~	~~50~~	~~100~~	~~200~~		~~32.3~~

Table 5 shows the same match-up information as in Table 4, but for SPS. We would like to highlight again, the SPSs proposed by Yang et al (2013) are used for the radiative transfer calculation. From a single ice crystal point of view, those shapes are very unlikely to occur exactly in reality. This is similar to the issue in field measurements. In field-based measurements, s~~S~~pherical shape assumption is widely used (e.g., the ~~measurement~~ calculation of SSA from SGS), however, a pure spherical shape is also very unlikely to occur in natural snow. To have a reasonable comparison between satellite-derived SPS and field-measured SPS, the quantitative information of „roundish" or „irregular" shapes from both satellite and field measurement communities may be an option. Under this comparison strategy, a „droxtal" shape derived from satellite observation is somehow identical with a „spherical shape" in field measurement.

The second and third column in Table 5 are SnowEx17-measured and XBAER-derived SPS. The abbreviations of the SPS are listed in Table 2. The 4-6th columns are the temperature, wetness of snow and the comments provided by campaign, respectively. Previous publications show that ice cloud and fresh snow are best described by aggregate of 8 columns (Platnick et al., 2017; Järvinen et al., 2018). Both 9th and 11th February are retrieved to be aggregate of 8 columns because both of them are affected by ice cloud. The first sample on 22nd February is reported to be aggregate of 8 columns and the observation of SnowEx17 is fresh snow. The SPS of the second sample on 22nd February is "facet" while XBAER says "droxtal" ~~(no exact facet shape is defined in Yang et al., 2013), both tend to be roundish~~, indicating possible linkage between XBAER derived "droxtal" and filed measured "facet". It is interesting to compare the SPS for the third sample on 22nd February. The SPSs are round and aggregate of 8 columns for SnowEx17 measurement and XBAER retrieval, respectively. The atmospheric condition is reported to be "windy" and the snow layer is wind-affected and not very well-banded ice crystal. Ice crystal shape in blowing snow is likely to be irregular and aggregated (Lawson et al., 2006; Fang and Pomeroy, 2009; Beck et al., 2018), which is strongly affected by the near surface processes (Beck et al., 2018). Snow grain may also get rounded due to sublimation in blowing snow (Domine, 2009). The wind blowing snow may be well-represented optically by a "aggregate of 8 columns" shape, as retrieved by XBAER.

Table 5 The comparison between SnowEx snow grain shape and XBAER retrieved SGP during February, 2017.

Date	SnowEx shape	XBAER shape	Temperature (°)	Wetness	Comment
02-09	Rounds	col8e	0.2	Wet	-
02-11	New Snow	col8e	-2.5	Middle	Storm snow, some grapple, some aggregation of crystals
02-22	New Snow	col8e	-5.1	Dry	Very surface has sparse surface hoar, affected by yesterday's warm up, bit of crust fragments
02-22	Facets	droxa	-3.6	Dry	Very very thin layer of tiny surface facets, still standing not well formed
02-22	Rounds	col8e	-1.8	Dry	Surface very wind-affected very thin (3mm) melt- freeze layer not very well-banded
02-11	New Snow	col8e	-2.5	Middle	Storm snow, some grapple, some aggregation of crystals

Table 6 shows the comparison of SSA. For the three cloud-free samples, the difference of XBAER-derived SSA and SnowEx17 measured SSA is 2.7 m^2/kg, which is significantly smaller than what has been reported by previous publications. For instance, the differences between satellite retrievals and field measurements are reported to be 9 m^2/kg and ~6 m^2/kg as presented in Mary et al (2013) and Xiong et al (2018). An interesting case is observed for the two-sample on 22nd February (samples 3 and 4). The SGSs show the same values for these two match-ups (both are 254.4 µm from XBAER and 250 µm from SnowEx), however, ground-based measurement shows almost two times the difference of SSA (29.8 m^2/kg vs 14.6 m^2/kg) for these two samples, which is due to the different SPSs. SnowEx shows that the SPSs are new snow and facets for these two samples, respectively. XBAER derived SSAs are 24.5 and 12.9 m^2/kg, which agrees well with SnowEx measurement. Since both SnowEx and XBAER provide very similar SGS (250 µm vs 254.4 µm), the agreement of SSA indicates that XBAER derived “aggregate of 8 columns“ is comparable to „new snow“ while XBAER derived „droxtal“ is somehow „identical“ to “facets” in SnowEx. Cloud contamination introduces an overestimation of SSA, especially for 11th February. According to the investigation from the companion paper, for reference SSAs of 37.3 and 25.9 m^2/kg, SSA is expected to be ~ 65 m^2/kg and >100 m^2/kg for cloud contamination with COT ~ 0.5 and 10, respectively. The real satellite retrieval values are 56.5 and 136.8 m^2/kg, respectively.

Table 6 The comparison between SnowEx SSA and XBAER retrieved SSA during February, 2017.

Date	Lon(°)	Lat(°)	SnowEx(m^2/kg)	XBAER(m^2/kg)
02-09	-108.1092	39.0369	37.3	56.5
02-11	-108.0462	39.0278	25.9	136.8
02-22	-108.0634	39.0444	18.5	17.4
02-22	-108.0625	39.0459	14.6	12.9
02-22	-108.0617	39.047	29.8	24.5
02-11	-108.0462	39.0278	25.9	136.8

The above validation for the retrieval of SGS, SPS, and SSA using the XBAER algorithm, although with limited samples, indicate the consistent of the sensitivity study from the companion paper in part 1 and the retrieval results in part 2, as presented in this section.

5.2 Validation using the observations of other campaigns

For a comprehensive validation, we have analyzed the rest of the sites beside the SnowEx site. The comparison is peformed based on the daily mean observation following the method from Wiebe et al. (2011). We have restircted the SGS in the range of 0 – 300 μm while the SSA is in the range of 0 – 100 m^2/kg. Thus there may be a slightly difference in the number of total match-up numbers for SGS and SSA. Fig. 8 shows the comparison between XBAER derived snow properties and field-based measurements. Both SGS and SSA show good correlation between XBAER derived and field-based measurements, with correlation coeffcients larger than 0.85. A clear underestimation of SGS, especially for large SGS values, is observed. This can also been seen from the slope of the regression (slope = 0.67). XBAER shows good agreement with field-based measurements, especially for SGS smaller than 150μm. The underestimation occurs mainly over regions with complicated surface condition and/or large aerosol loading. In general, we can see larger deviation to the 1:1 line when AOT values are larger. This agrees with a major finding in Part 1 of the companion paper, that is aerosol contaminaton introduces underestimation of SGS. For instance, large AOT values can be seen over China, while strong underestimation of SGS is also observed. For Alps and two canadian (Canada-Alex, Canada-Josh) sites, the AOT values are farily low, the underestimation may be explained by the strong surface inhomogeneity (possibly due to different surface types in one satelite pixel). For site Greenland and Antarctica, where AOT values are low and surface is covered mainly by snow, XBEAR shows good performance. This can be confirmed by the RMSE values. The RMSE values in Fig. 8 are calculated only for site Greenland and Antarctica, to avoid the large outliners over other sites (please be noted other sites provide quite limited number of match-ups, see Fig. 9). The RMSE value is 12 μm.

The comparsion between XBAER derived and field-measured SSA shows no significant under/over-estimation (slope = 1) with correlation coeffcient R = 0.93. XBAER derived SSAs are, in general, larger than field-based measurements. This can be explained by the use of different SPS assumptions. In the XBAER algorithm, for the match-ups shown in Fig. 8, most SPSs are non-convex while the convex SPS is used for field-measured values. We recall, that for the same SGS, non-convex particle leads to a larger SSA, compared to convex particle. The impact of aerosol contamination, compared to surface condition, seems to play a major role of the observed overestimations.

The potential linkage beween XBAER derived SPS and filed-measured SPS is also presented in Fig. 8. This is named as SPS similarity in this manuscript. The SPS similarity is defined as the ratio of match-up number for a given SPS pair (XBAER retrieved Yang SGS, field measured ICSSG SPS) to the total match-up number. The higher SPS similarity, the higher chance this SPS pair may occur in reality, indicating the higher possibility of the retrieved Yang SPS may have closer relationship with ICSSG SPS. According to Fig. 8, we can see that aggregate of 8 columns, solid bullet rosettes and column show stronger linkage with the rounded grains while droxtal, plate and column show stronger linkage with the faceted crystals. This may lead to some imperfect and highly uncertain linkage between XBAER derived SPS and the ICSSG SPS. Aggregate SPS in XBAER is likely to be matched with rounded gains while single SPS in XBAER is possibly linked to faceted crystals. There are also possible linkage between XBEAR SGS and ICSSG SPS, for instance, aggregate of 8 columns and plate with precipitation particles, solid bullet rosettes with depth Hoar, droxtal and plate with surface hoar. The above linkage also indicates that aggregate of 8 columns (linked to rounded grains and precipitation particles) may represent fresh snow while droxtal (linked to faceted crystals and surface hoar) may represent aged snow. This agrees with the previous analysis over Greenland.

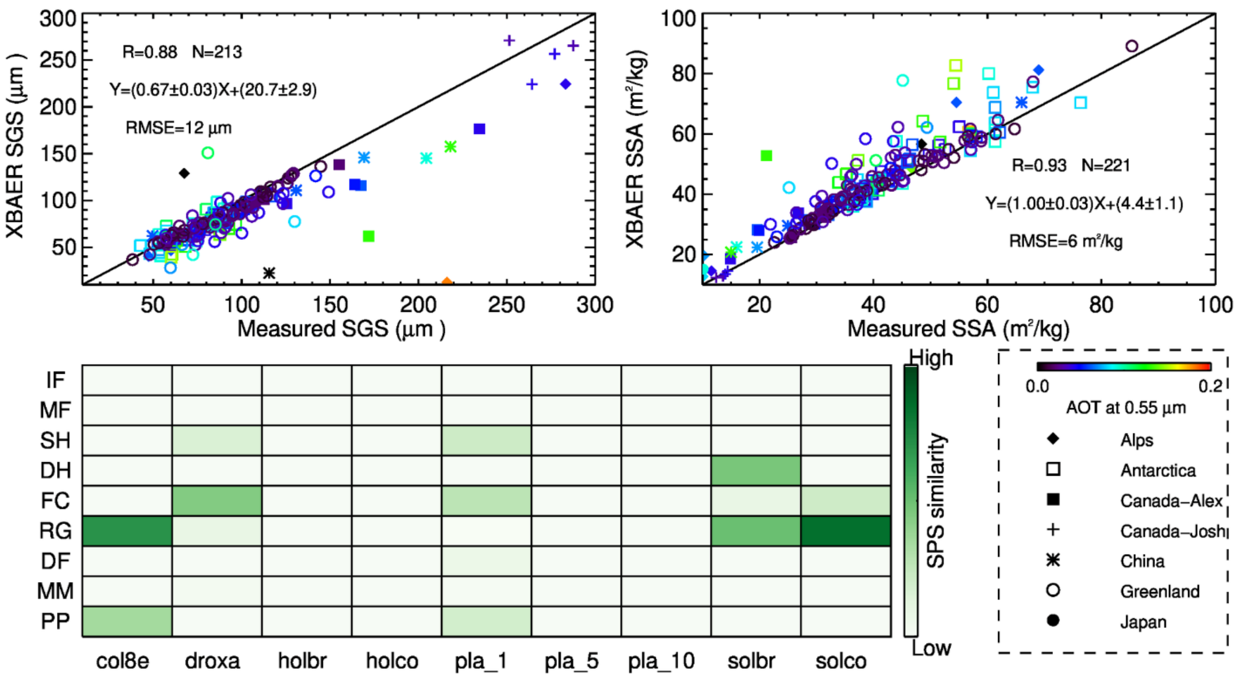

Fig 8 Validation of XBAER derived SGS, SPS and SSA. The upper panel shows the scattering plot for SGS and SSA, while the lower panel shows the relationship of SPS between XBAER and ICSSG. The match-ups for SGS and SSA are distinguished by sites and the AOT. The correlation coefficient (R), number of match-ups (N), the regression equation, and the RMSE are given. The relationship of SGS between XBAER and ICSSG (named as SPS similarity) is defined as the ratio of the number given match-ups to the total match-ups.

Fig. 9 and Fig. 10 show the time series of SGS and SSA over each site. We can see that sites Greenland and Antarctica provide most of the match-ups. Both SGS and SSA show good agreement between XBAER derived and field measured values over these two sites. For SGS, the correlation coefficients are 0.85 and 0.89, the RMSEs are 14 and 9 µm, respectively. For SSA, those values are 0.84, 0.89 for correlation coefficient and 8 and 7 m^2/kg for RMSE, respectively. Although the other sites provide limited match-ups, they still give helpful information for the understanding of impacts of surface and atmospheric conditions. In general, sites China and Japan show large AOT values, leading to underestimation of SGS and overestimation of SSA. For two Canadian sites (Canada-Alex, Canada-Josh), the under/over-estimation of SSA and SGS may largely explained by the surface condition. Site Alps seems to be affected by both surface and atmospheric impacts.

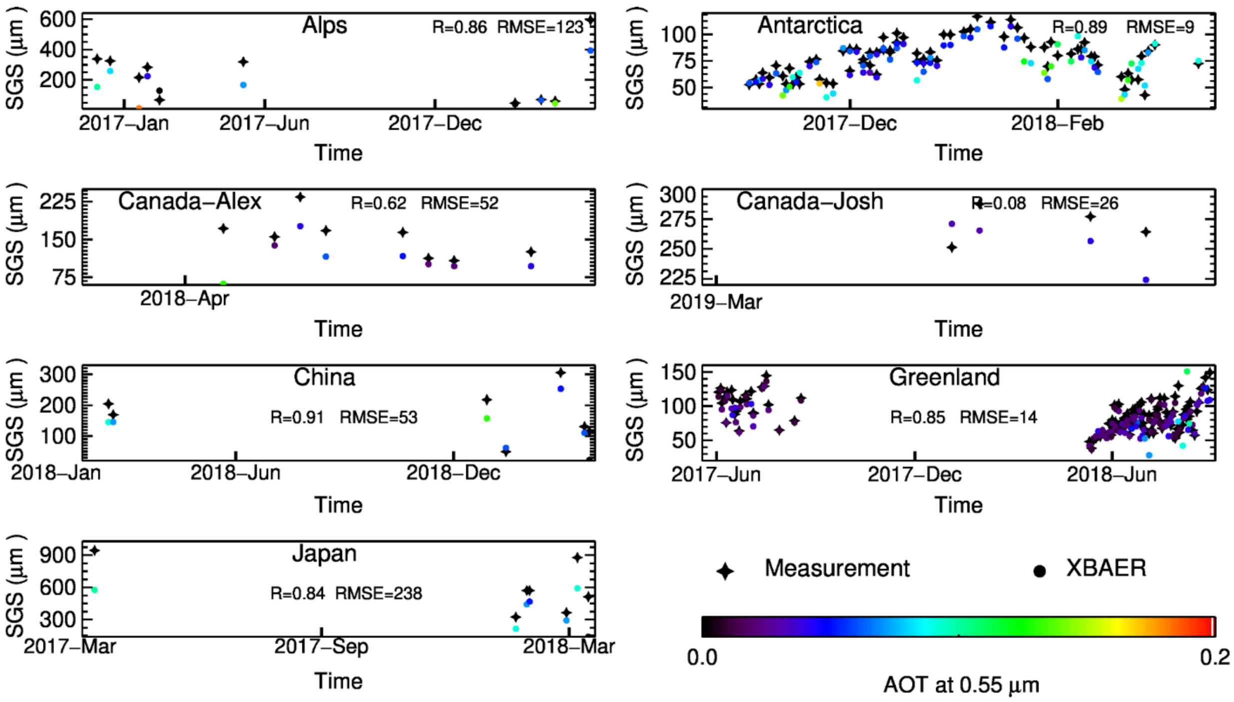

Fig 9 Time series of XBAER derived and field-measured SGS for each site. The match-ups for SGS are distinguished by the AOT values. The correlation coefficient (R) and the RMSE are given.

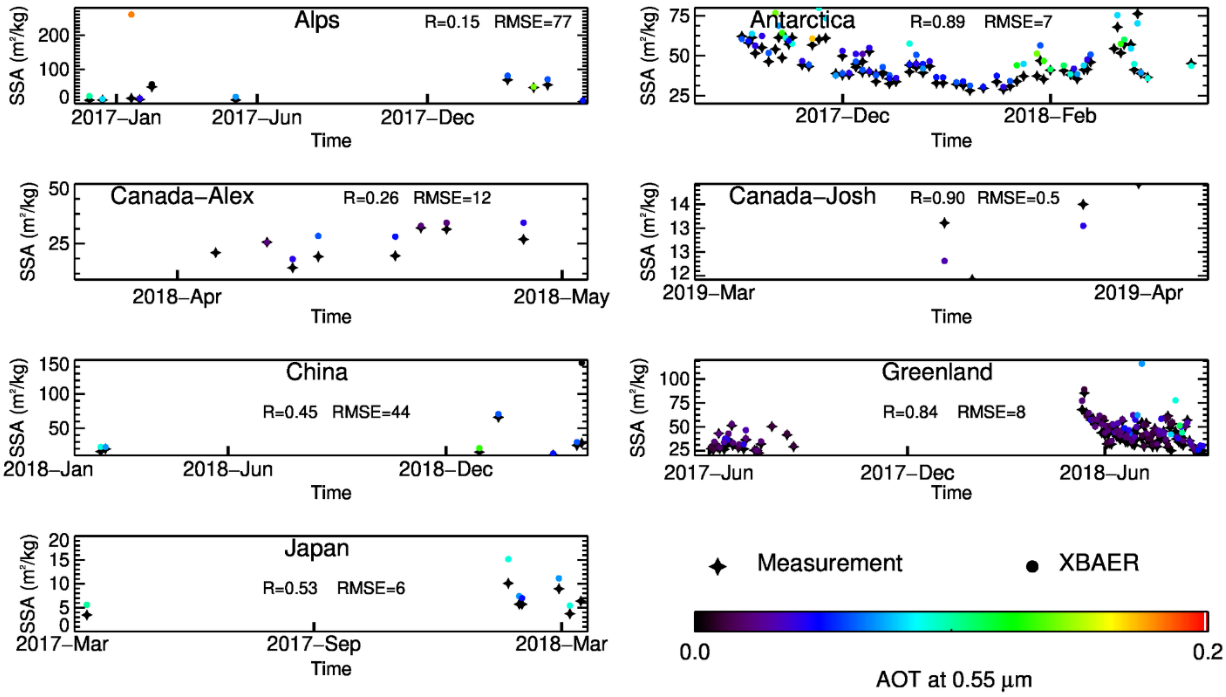

Fig 10 Time series of XBAER derived and field-measured SSA for each site. The match-ups for SGS are distinguished by the AOT values. The correlation coefficient (R) and the RMSE are given.

5.~~2~~ 3 ~~Comparison with~~Validation using the observations of aircraft campaign

The optical snow grain size over Arctic sea ice was derived from airborne SMART measurements as described in Sect. 2.3. Fig. ~~6~~ 11 (a) shows the retrieved grain size along the flight track (black encircled area) taken on 26 March 2018 between 12 and 14 UTC north of Greenland. During this period of cloudless conditions, a Sentinel3 overpass (12:29 UTC) delivered SGS data based on the XBAER algorithm as displayed in the background of this map with 1 km spatial resolution. In general, lower SGS were observed by both methods in the vicinity of Greenland, while in particular in the North-East region of the map (red dashed circle in Fig. ~~6~~ 11 (a)) SGS values of up to 350 µm were derived from the aircraft albedo measurements. Also the XBAER algorithm reveals higher values in this region. For a direct comparison XBAER data were allocated to the time series of the SMART measurements along the flight track. Afterwards all successive SMART data points assigned to the same XBAER location were averaged to compile a joint time series of both data sets as displayed in Fig. ~~6~~ 11 (b). Overall a correlation coefficient of R = 0.82 and a root mean squared error of RMSE = 12.4 µm was derived, where SMART (mean SGS: 165±40 µm) generally shows ~~lower~~ higher grain sizes than XBAER (mean SGS: 138±21 µm). The course of the SGS follows a similar pattern for both methods, with largest deviations when the aircraft measured in the red dashed circled area from Fig. ~~6~~ 11 (a). The corresponding time periods are indicated by the light red shaded area. Camera observations along the flight track have revealed an increase of surface roughness in this area. Note, that the flight altitude varied for the flight section shown in Fig. ~~6~~ 11 (a). Due to the low sun, such a non-smooth surface produces a significant fraction of shadows which lowers the measured albedo. Consequently, the retrieved SGS is affected in particular for the lowest flight section when SMART collects the reflected radiation with high spatial resolution. This might explain why the deviation of the retrieved SGS values in this area are largest around 13 UTC when flight altitude was in the range of 100 m.

The SGS retrieval based on the algorithm suggested by Zege et al. (2011) and Carlsen et al. (2017) give the optical radius of the snow grains, such that the SSA can be derived applying Eq. (A1) from companion paper. The map of the SSA (Fig. ~~6~~ 11 (c)) reflects a similar pattern than observed for the SGS, showing an inverse behavior to Fig. ~~6~~ 11 (a). In average, XBAER (mean SSA: 24±3 m^2/kg) and SMART (mean SSA: 21±5 m^2/kg) agree within the 1-sigma standard deviation. The correlation of SSA between XBAER and SMART is similar as for the SGS with a correlation coefficient R = 0.81 and RMSE = 2.0 m^2/kg. A comprehensive comparison between XBAER and SMART is given in Jake et al. (2021).

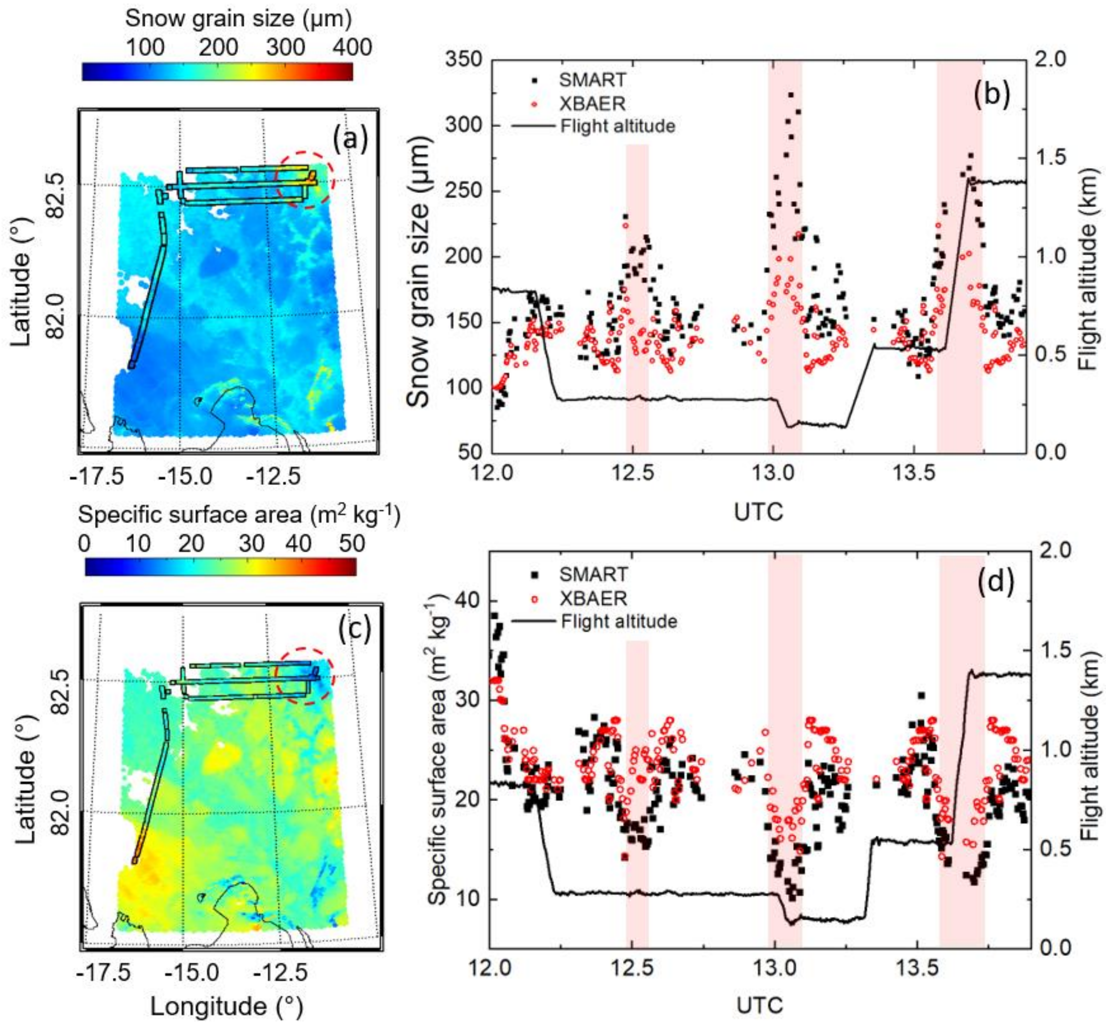

Figure ~~6~~11: (a) Map of SGS retrieval results from Sentinel measurements in the North of Greenland from 26 March 2018. The black encircled area represent the SMART retrievals of the SGS along the flight track. The red dashed circle marks a region with increased surface roughness. (b) Time series of both retrieval data sets adapted to the aircraft flight path. Periods matching with the circled area in (a) are shaded in light red. (c) and (d) are similar to (a) and (b) but for SSA. Additionally, the flight altitude is given.

Since XBAER is also designed to support MOSAiC campaign on an Arctic-wide scale (Mei et al., 2020c), it is important to have an overview of how snow properties look like on an Arctic-wide scale for existing campaign. Fig. ~~7~~ 12 shows the SGS, SPS and SSA geographic distribution over the whole Arctic for 26 March 2018. Northern Greenland, North America, and central Russia show large snow particles, especially over North America. And the SPS shows more diversities in lower latitude compared to the central Arctic, indicating stronger SPMP. An aggregated shape such as aggregate of 8 columns is the dominant shape in the central Arctic while column is one of the dominant shapes in lower latitude. SSA shows large values in the lower latitude Arctic (northern Canada, southern Greenland, western Norway, southern Finland, northern Russia) while the values are smaller in the central Arctic.

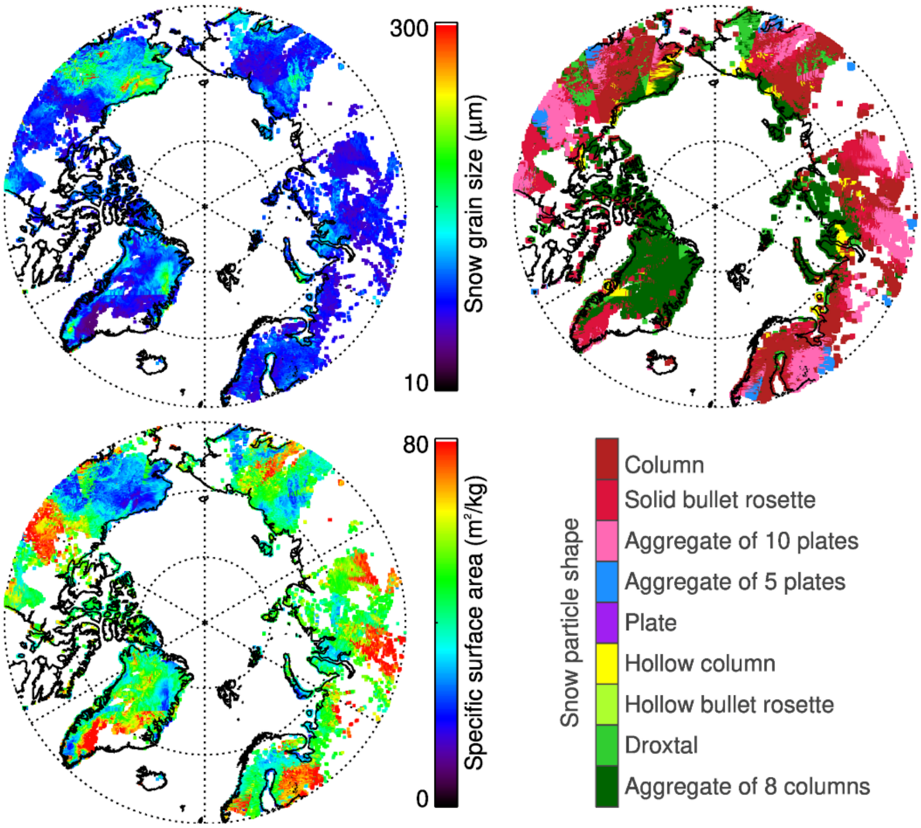

Fig. ~~7~~ 12 The distribution of XBAER-derived SGS, SPS and SSA over the whole Arctic for 26 March 2018

6 Discussion

The above analysis shows the promising quality of XBAER-derived SGS, SPS and SSA results. The XBAER retrieved SGS, SPS and SSA can be used to understand the change of snow properties temporally. Even though the snow metamorphism depends on the environmental conditions, Aoki et al. (2000) and Saito et al. (2019) pointed out that a 4-days time scale is a reasonable time-span to see the temporal change of snow properties. Fig. ~~8~~ 13 shows XBAER-derived SGS (upper panel), SPS (middle panel) and SSA (lower panel) over Greenland during 27 – 30 July, 2017. Large variability for SGS, SPS and SSA can be seen during these four days, indicating the impacts of snow metamorphism on the snow properties. Fig. ~~8~~ 13 shows snow melting process in both western and northeastern parts of Greenland, especially during 28 July. The strong melting in July over Greenland has also been reported by Lyapustin et al (2009). SPS over southeastern part of Greenland becomes smaller during those four days. No snowfall has been reported according to POLAR PORTAL report (http://polarportal.dk/en/greenland/surface-conditions/) during these four days, thus the smaller SGS may be caused by local snow metamorphism process and/or due to the wind-blown fresh snow, transported from central Greenland to southeastern parts. This is consistent with the wind direction as presented in Fig. 14~~reported as https://www.windy.com/?62.083,2.900,4~~. The wind speed is over 6 m/s, which is strong enough to blow the surface ice crystal up. However, possible cloud containmination over northwest of Greenland may occur, leading to very small SGS. The change of SGS is also consistent with the change of SPS. Please be noted, since the SGS and SPS are retrieved simultaneously, the selection of different SPSs leads to a different SGS, thus the change of SGS and SPS with respect to time may also be affected by the algoritm itself. According to Fig. ~~8~~13, SPSs over Greenland derived from the XBAER algorithm are mainly droxtals and solid bullet rosettes for the selected days. The solid bullet rosettes and droxtal are typical ice crystal shapes for fresh snow and aged snow (Nakamura et al.,2001), respectively. The wind-blown fresh snow might be transported to the eastern part of Greenland, and fresh snow covers the original aged snow, thus a solid bullet rosettes shape is retrieved. According to Fig. 8, droxtals and solid bullet rosettes retrieved by XBAER may link to faceted crystals and rounded grains in ICSSG, respectively. During the transport, faceted crystals turn into rounded grains. The change of SSA follows the change of SGS and SPS. SSA over central Greenland is larger while it is smaller in the coastline regions. This can be explained by the reduced SPMP impact on the snow properties due to the increase of elevation in central Greenland. Inversely proportional to SGS, the SSA reduces. The coverage of large SSA over the eastern part of Greenland increase during these four days, indicating the "~~„~~snowfall” feature due to transport. This wind-induced transport feature, similar to fresh snowfall, changes both

SGS and SPS. And this process is revealed by and superimposed on the SPMP during the temporal change of SSA retrieved from satellite observations (Carlsen et al., 2017).

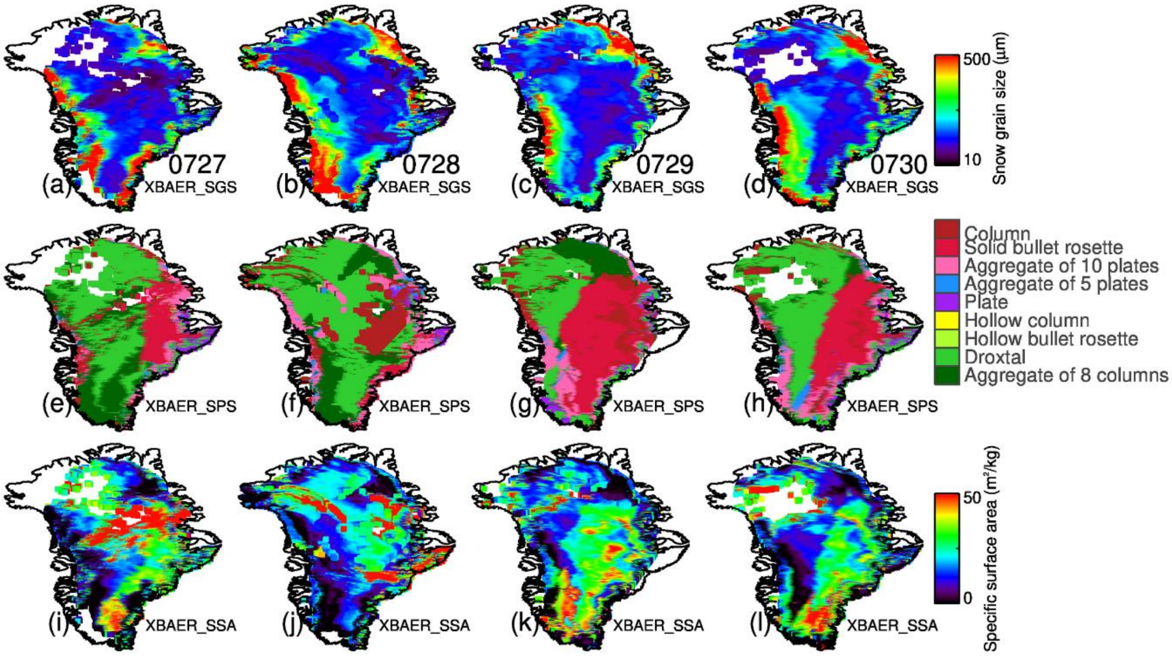

Fig ~~8~~13. XBAER derived SGS, SPS and SSA over Greenland during 27 – 30 July 2017.

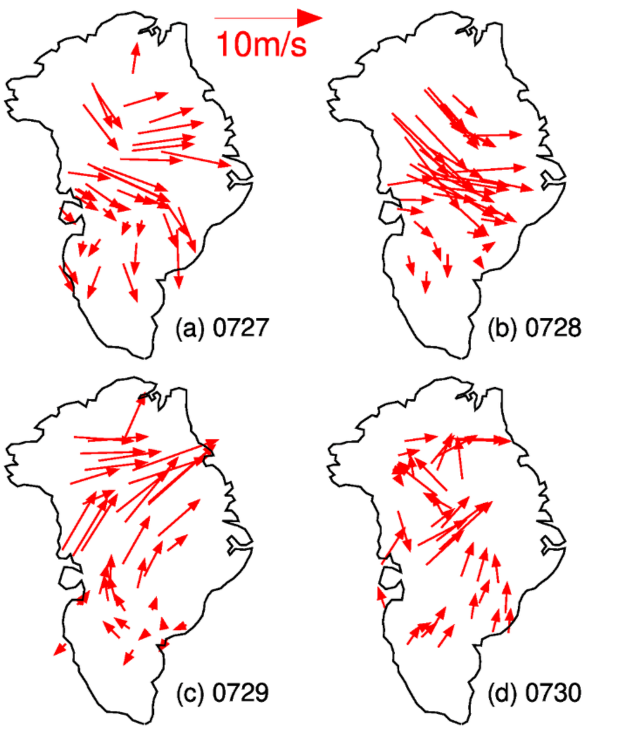

Fig 14. Wind direction (reference to North) and wind speed (unit: m/s) over Greenland during 27 – 30 July 2017.

7 Conclusions

SGS, SPS and SSA are three important parameters to describe snow properties. Both SGS, SPS and SSA play important roles in the changes of snow albedo/reflectance, further impact the atmospheric and energy-exchange processes. A better knowledge of SGS, SPS and SSA can provide more accurate information to describe the impact of snow on Arctic amplification processes. The information about SGS, SPS and SSA may also explore new applications to understand the atmospheric conditions (e.g. aerosol loading). Although some previous attempts (e.g. Lyapustin et al., 2009) show the capabilities of using passive remote sensing to derive SGS over a large scale, no publications have been found to derive SGS, SPS and SSA simultaneously. This is the first paper, to our best knowledge, attempting to retrieve both SGS, SPS and SSA using passive remote sensing observations.

The new algorithm is designed within the framework of XBAER algorithm. The XBAER algorithm has been applied to derive SGS, SPS and SSA using the newly launched SLSTR instrument onboard Sentinel-3 satellite. The cloud screening is performed with a synergistical technique using both OLCI and SLSTR measurements. ~~The synergistical usage of OLCI and SLSTR explore the maximum wavelength information provided by both instruments. The O_2-A channel in OLCI and infrared channel in SLSTR instrument provide valuable information to detect cloud over snow surfaces. The use of OLCI and SLSTR, rather than SLSTR alone, show good performance of cloud screening compared to previous publications (e.g Istomina et al., 2010).~~ The synergistical cloud screening in XBAER is easy-implementable and effective-runable on a global scale, with high-quality, enables a cloud-contamination-minimized SGS, SPS and SSA retrieval using passive remote sensing.

Besides the cloud screening, another pre-process is the atmospheric correction. Aerosol plays a non-ignorable impact on the retrieval of SGS, SPS and SSA, even over the Arctic regions, where aerosol loading is small (AOT, at 0.55µm is around 0.05) (Mei et al., 2020b). In the XBAER algorithm, the MERRA simulated AOT at 0.55µm, together with a weakly absorption aerosol type (Mei et al., 2020b) is used as the inputs for the atmospheric corrections.

The SGS, SPS and SSA retrieval algorithm is based on the publication by Yang et al (2013), in which a database of optical properties for nine typical ice crystal shapes ~~(aggregate of 8 columns, droxtal, hollow bullet rosettes, hollow column, plate, aggregate of 5 plates, aggregate of 10 plates, solid bullet rosettes, column)~~ are provided. Previous publications show that this database can be used to retrieve ice crystal properties in both ice cloud and snow layer (e.g.,Järvinen et al., 2018; Saito et al., 2019). The algorithm is a LUT-based approach, in which the minimization is achieved by the comparison between atmospheric corrected TOA reflectance at 0.55 and 1.6 µm observed by SLSTR and pre-calculated LUT under different geometries and snow properties. The retrieval is relatively time-consuming because the minimization has to be performed for each ice crystal shape and the optimal SGS and SPS are selected after the 9 minimizations are done. The SSA is then calculated using the retrieved SGS and SPS based on another pre-calculated LUT.

The comparison between XBAER derived SGS, SPS and SSA show good agreement with the SnowEx17 campaign measurements. The average absolute and relative difference between XBAER derived SGS and SnowEx17 measured SGS is about 10 µm and 4%, respectively. XBAER derived SGS also shows good agreement with MODIS SGS product. XBAER retrieved SPS reveals reasonable and explainable linkage with SnowEx17 measurements. The difference of XBAER-derived SSA and SnowEx17 measured SSA is 2.7 m^2/kg. The retrieval results over Greenland reveal the general patterns of snow properties over Greenland, which is consistent with previous publications (Lyapustin et al. 2009). ~~SGS is smaller over central Greenland and larger over coastline regions due to the meteorological conditions. The spatial distribution of SSA is somehow anti-correlated with SGS. The fresh snow and aged snow over Greenland are well-captured by droxtals and solid bullet rosettes.~~ The change of SGS, SPS and SSA on a 4 days time span is also observed using XBAER retrieved SGS, SPS and SSA. The comparison with aircraft measurement during PAMARCMiP campaign held in March 2018 also indicates good agreement (R = 0.82 and R=0.81 for SGS and SSA, respectively), XBAER-derived SGS and SSA reveal the variabilities of the aircraft track of the PAMARCMiP campaign. ~~XBAER-derived SGS/SSA show smoother patterns compared to aircraft measurements due to spatial resolution, height, and observation geometries. XBAER derived SGS, SPS and SSA over the whole Arctic for the aircraft measurement period show strong variabilities for SGS, SPS and SSA.~~A intensive validation is performed using seven addtional field-based measurements. XBAER derived SGS and SSA show high correlation with field measurements, with correlation coeffcients are higher than 0.85. The RMSE for SGS and SSA are less than 15 µm and 10 m^2/kg, respectively. The validation of SPS reveals that XBEAR derived aggregate SPS is likely to be matched with rounded grains while a single SPS in XBAER is possibly linked to faceted crystals in the ICSSG classification. This possible linkage, although inaccurate, will be helpful to understand the snow properties in a large scale.

Although the presented version of the XBAER retrieval algorithm shows promising results, we see at least ~~three~~ four possibilities to improve its accuracy. ~~An intensive validation with the support of MOSAiC campaign is needed.~~ Potential cloud contamination may still occur according to the analysis, exploiting the time-series technique, as described in Jafariserajehlou et al. (2019). Currently only single ice crystal shape is used in the retrieval, the mixture of different ice crystal shapes i.e., the snow grain habit mixture model (e.g., Saito et al. 2019) will be tested in further work. Another potential improvement may be linked to the us~~ag~~e of polydisperse ice crystals (e.g. gamma distribution). The potential impacts of the vertical structure of SGS and SPS also need to be investigated in the future.

XBAER-derived SGS, SPS, and SSA will be used to support the analysis of MOSAiC ~~(Multidisciplinary drifting Observatory for the Study of Arctic Climate)~~ expedition and other campaign-based measurements (Jake et al., 2021).

Code and data availability

The data over Antarctica site is provided by Dr. Ghislain Picard. The data over site Greenland site is provided by Dr. Hans Christian Steen-Larsen. The data over site Canada-Alex site is provided by Dr. Alexandre Langlois. The data over Canada-Josh site is provided by Dr. Joshua

King. The data over China site is provided by Dr. Tao Che. The data over Japan site is available at https://doi.pangaea.de/10.1594/PANGAEA.909880. The data over Alps site is available at https://perscido.univ-grenoble-alpes.fr/datasets/DS330. The data over SnowEx site is available at https://nsidc.org.

Author contributions

LM and VR conceptualized the study, LM implemented the code and processed the data. LM, VR EJ, XC analyzed the data. LM prepared he manuscript with contribution from all co-authors. LM, VR, MV and JB polished the whole manuscript.

Competing interests

The authors declare that they have no conflict of interest.

Acknowledgements

This research was funded by the Deutsche Forschungsgemeinschaft (DFG, German Research Foundation) – Project-ID 268020496 – TRR 172. The comments by Dr. Alexandre Langlois, Dr. Ghislain Picard and the anonymous reviewer help to improve the quality of the manuscript significantly. The authors highly appreciate the effort from Dr. Adam Povey (University of Oxford) to help to deal with the huge amount of the SLSTR L1 data. The authors would like to thank Prof. Knut von Salzen from Environment Canada for the valuable discussion. We thank the support from Dr. Lisa Booker from National Snow and Ice Data Center, Boulder to understand the SnowEx17 campaign data. We thank Dr. Alexander Kokhanovsky from

VITROCISET, Darmstadt, Germany and Prof. Jason E. Box from Geologic Survey of Denmark and Greenland (GEUS) for the valuable discussion. We thank Salguero Jaime for providing the MODSCAG snow products. The MODIS snow product data are provided by MODSCAG team and SLSTR/OLCI data are provided by ESA.

Reference

Aoki, T., Aoki, T., Fukabori, M., and Uchiyama, A.: Numerical simulation of the atmospheric effects on snow albedo with a multiple scattering radiative transfer model for the atmosphere-snow system, *J. Meteor. Soc. Japan*, 77, 595–614, https://doi.org/10.2151/jmsj1965.77.2_595, 1999.

Aoki, T., Fukabori, M., Hachikubo, A., Tachibana, Y., and Nishio, F.: Effects of snow physical parameters on spectral albedo and bidirectional reflectance of snow surface, *J. Geophys. Res.*, 105(D), 10 219–10 236, 2000.

Aoki, T., Hori, M., Motoyoshi, H., Tanikawa, T., Hachikubo, A., Sugiura, K., Yasunari, T., Storvold, R., Eide, H., Stamnes, K., Li, W., Nieke, J., Nakajima, Y. and Takahashi, F.: ADEOS-II/GLI snow/ice products - part II: Validation results using GLI and MODIS data, *Remote Sens. Environ.*, 111:274–290. doi: 10.1016/j.rse.2007.02.035, 2007.

Avanzi, F., Johnson, R.C., Oroza, C.A., Hirashima, H., Maurer, T., Yamaguchi, S.: Insights into preferentialflow snowpack runoffusing random forest, *water resources research*, 55(12), 10727 – 10746, 2019

Barnett, T. P., Adam, J. C. and Lettenmaier, D. P.: Potential impacts of a warming climate on water availability in snow-dominated regions. *Nature* 438, 303–309, 2005.

Beck, A., Henneberger, J., Fugal, J. P., David, R. O., Lacher, L., and Lohmann, U.: Impact of surface and near-surface processes on ice crystal concentrations measured at mountain-top research stations, *Atmos. Chem. Phys.*, 18, 8909–8927, https://doi.org/10.5194/acp-18-8909-2018, 2018.

Bokhorst, S., Pedersen, S.H., Brucker, L. et al.: Changing Arctic snow cover: A review of recent developments and assessment of future needs for observations, modelling, and impacts. *Ambio*, 45, 516–537. https://doi.org/10.1007/s13280-016-0770-0, 2016.

Brucker, L., Hiemstra, C., Marshall, H.-P., Elder, K., De Roo, R., Mousavi, M. , Bliven, F., Peterson, W., Deems, J., Gadomski, P., Gelvin, A., Spaete, L., Barnhart, T., Brandt, T., Burkhart, J., Crawford, C., Dutta, T., Erikstrod, H., Glenn, N., Hale, K., Holben, B., Houser, P., Jennings, K., Kelly, R., Kraft, J., Langlois, A., McGrath, D., Merriman, C., Molotch, N. and Nolin, A.: A first overview of SnowEx ground-based remote sensing activities during the winter 2016–2017, *2017 IEEE International Geoscience and Remote Sensing Symposium (IGARSS)*, 1391-1394, doi: 10.1109/IGARSS.2017.8127223, 2017.

Chandrasekhar, S.: Raditive Transfer. London: Oxford University Press, 1950

Chen, T., Pan, J., Chang ,S., Xiong, C., Shi, J., Liu, M., Che, T., Wang, L. And Liu, H., validation of the SNTHERM model applied for snow depth, grain size, and brightness temprature simulation at meteorological stations in China, *Remote Sensing*, 12 (3), 507, 2020

Carlsen, T., Birnbaum, G., Ehrlich, A., Freitag, J., Heygster, G., Istomina, L., Kipfstuhl, S., Orsi, A., Schäfer, M., and Wendisch, M.: Comparison of different methods to retrieve optical-equivalent snow grain size in central Antarctica, *The Cryosphere*, 11, 2727–2741, https://doi.org/10.5194/tc-11-2727-2017, 2017.

Colbeck, S. C.: Thermodynamics of snow metamorphism due to variations in curvature, *J. Glaciol.*, 26, 291-301, 10.3189/S0022143000010832, 1980.

Colbeck, S. C.: Theory of metamorphism of dry snow, *J. Geophys. Res.*, 88, 5475-5482, 1983.

Cohen, J., and D. Rind: The Effect of Snow Cover on the Climate. *J. Climate*, 4, 689–706, https://doi.org/10.1175/1520-0442(1991)004<0689:TEOSCO>2.0.CO;2, 1991

Cole, B. H., Yang, P., Baum, B. A., Riedi, J., and C.-Labonnote, L.: Ice particle habit and surface roughness derived from PARASOL polarization measurements, *Atmos. Chem. Phys.*, 14, 3739-3750, https://doi.org/10.5194/acp-14-3739-2014, 2014.

Comola, F., Kok, J. F., Gaume, J., Paterna, E., and Lehning, M.: Fragmentation of wind-blown snow crystals, *Geophys. Res. Lett.*, 44, 4195–4203, https://doi.org/10.1002/2017GL073039, 2017GL073039, 2017.

Dang, C., Fu, Q., and Warren, S. G.: Effect of snow grain shape on snow albedo, *J. Atmos. Sci.*, 73, 3573–3583, https://doi.org/10.1175/JAS-D-15-0276.1, 2016.

Dumont, M., Brissaud, O., Picard, G., Schmitt, B., Gallet, J.-C., and Arnaud, Y.: High-accuracy measurements of snow Bidirectional Reflectance Distribution Function at visible and NIR wavelengths – comparison with modelling results, *Atmos. Chem. Phys*., 10, 2507-2520, https://doi.org/10.5194/acp-10-2507-2010, 2010.

Egerer, U., Gottschalk, M., Siebert, H., Ehrlich, A., and Wendisch, M.: The new BELUGA setup for collocated turbulence and radiation measurements using a tethered balloon: first applications in the cloudy Arctic boundary layer, *Atmos. Meas. Tech*., 12, 4019–4038, https://doi.org/10.5194/amt-12-4019-2019, 2019.

Elder, K., L. Brucker, C. Hiemstra, and H. Marshall. : *SnowEx17 Community Snow Pit Measurements, Version 1*. [Indicate subset used]. Boulder, Colorado USA. NASA National Snow and Ice Data Center Distributed Active Archive Center. doi: https://doi.org/10.5067/Q0310G1XULZS. [Date Accessed], 2018.

Fang, X. and Pomeroy, J. W.: Modelling blowing snow redistribution to Prairie wetlands, *Hydrol. Process*., 23, 2557–2569, doi:10.1002/hyp.7348, 2009.

Flanner, M. G. and Zender, C. S.: Linking snowpack microphysics and albedo evolution, *J. Geophys. Res.*, 111, D12208, doi:10.1029/2005JD006834, 2006.

Flanner, M., Shell, K., Barlage, M. et al.: Radiative forcing and albedo feedback from the Northern Hemisphere cryosphere between 1979 and 2008. N*ature Geosci.*, 4, 151–155, https://doi.org/10.1038/ngeo1062, 2011.

Fierz C., Armstrong, R.L., Durand, Y., Etchevers, P., Greene, E., McClung, D.D., Nishimura, K., Satyawali, P.K. and Sokratov, S.A.: The International Classification for seasonal snow on the ground, IHP-VII Technical Documents in Hydrology N°83, IACS Conribution N°1, UNESCO-IHP, Paris, 2009.

Gallet, J.-C., Domine, F., Zender, C.S., and Picard, G.: Measurement of the specific surface area of snow suing infrared reflectance in an integrating sphere at 1310 and 1550 nm, The cryosphere, 3 , 167 – 182, 2009.

Gastineau, G., J. García-Serrano, and C. Frankignoul: The Influence of Autumnal Eurasian Snow Cover on Climate and Its Link with Arctic Sea Ice Cover. *J. Climate*, 30, 7599–7619, https://doi.org/10.1175/JCLI-D-16-0623.1, 2017.

Groot Zwaaftink, C. D., Löwe, H., Mott, R., Bavay, M., and Lehning, M.: Drifting snow sublimation: A high-resolution 3-D model with temperature and moisture feedbacks. *Journal of Geophysical Research*, 116(D16). doi:10.1029/2011jd015754, 2011.

Gordon, M. and Taylor, P. A.: The Electric Field During Blowing Snow Events, *Bound-lay. Meteorol.*, 130, 97–115, 2009.

Hansen J., Lacis, A., Rind D., Russel G., Stone P., Fung I., Ruedy R., Lerner J.: Climate sensitivity: analysis of feedback mechanisms. *Clim. Process. Clim. Sensit*. (AGU Geophys. Monogr. Ser. 29) 5, 130–163, 1984.

Henderson, G.R., Peings, Y., Furtado, J.C. et al.: Snow–atmosphere coupling in the Northern Hemisphere. *Nature Clim Change*, 8, 954–963, https://doi.org/10.1038/s41558-018-0295-6, 2018.

Hori, M., Aoki, T., Stamnes, K. and Li, W.: ADEOS-II/GLI snow/ice products - part III:retrieved results, *Remote Sens. Environ.*, 111:291–336. doi: 10.1016/j.rse.2007.01.025, 2007.

Hyvarinen, T. and Lammasniemi, J.: Infrared measurement of free–water content and grain size of snow, *Opt. Eng*., 26(4), 342–348, 1987.

Ishimoto, H., Adachi, S., Yamaguchi, S., Tanikawa, T., Aoki, T. and Masuda, K. : Snow particles extracted from X-ray computed microtomography imagery and their single-scattering properties, *J. Quant. Spectrosc. Radiat. Transfer*, 209, 113–128, https://doi.org/10.1016/j.jqsrt.2018.01.021, 2018.

Istomina, L. G., von Hoyningen-Huene, W., Kokhanovsky, A. A., and Burrows, J. P.: The detection of cloud-free snow-covered areas using AATSR measurements, *Atmos. Meas. Tech.*, 3, 1005–1017, https://doi.org/10.5194/amt-3-1005-2010, 2010.

Järvinen, E., Jourdan, O., Neubauer, D., Yao, B., Liu, C., Andreae, M. O., Lohmann, U., Wendisch, M., McFarquhar, G. M., Leisner, T., and Schnaiter, M.: Additional global climate cooling by clouds due to ice crystal complexity, *Atmos. Chem. Phys.*, 18, 15767–15781, https://doi.org/10.5194/acp-18-15767-2018, 2018.

Jäkel, E., Mey, B., Levy, R., Gu, X., Yu, T., Li, Z., Althausen, D., Heese, B., and Wendisch, M.: Adaption of the MODIS aerosol retrieval algorithm using airborne spectral surface reflectance measurements over urban areas: a case study, *Atmos. Meas. Tech.*, 8, 5237–5249, https://doi.org/10.5194/amt-8-5237-2015, 2015.

Jeoung, H., Liu, G., Kim, K., Lee, G., and Seo, E.-K.: Microphysical properties of three types of snow clouds: implication for satellite snowfall retrievals, *Atmos. Chem. Phys.*, 20, 14491–14507, https://doi.org/10.5194/acp-20-14491-2020, 2020.

Jin, Z., Charlock, T. P., Yang, P., Xie, Y., and Miller, W. : Snow optical properties for different particle shapes with application to snow grain size retrieval and MODIS/CERES radiance comparison over Antarctica. *Remote Sensing of Environment*, 112(9), 3563–3581. doi:10.1016/j.rse.2008.04.011,2008

Kaufman, Y. J., Tanre, D., Remer, L. A., Vermote, E. F., Chu, A., and Holben, B. N.: Operational remote sensing of tropospheric aerosol over land from EOS moderate resolution imaging spectroradiometer. *Journal of Geophysical Research: Atmospheres*, 102(D14), 17051-17067, doi: 10.1029/96JD03988, 1997.

Key ,J., Mahoney, R., Liu, Y., Romanov, P., Tschudi, M., Appel, I., Maslanik, J., Baldwin,D.,Wang,X., Meade, P.: Snow and ice products from Suomi NPP VIIRS, *J. Geophys. Res.: Atmos.*, 118, 12816-12830, 2013.

Kikuchi, K., Kameda, T., Higuchi, K., and Yamashita, A.: A global classification of snow crystals, ice crystals, and solid precipitation based on observations from middle latitudes to polar regions, *Atmos. Res*., 132-133, 460–472, 2013.

King, J., Derksen, C., Toose, P., Montpetit, B. And Siqueira, P., TVCSnow: Seasonal Ku-band (13.25 GHz) SAR measurements in a snow-covered tundra basin, 76th Annual Eastern Snow Conference, Vermont, USA, June 2019

Kim, E., Gatebe, C., Hall, D., Newlin, J., Misakonis, A., Elder, K., Marshall, H., Hiemstra, C., Brucker, L., De Marco, E., Crawford, C., Kang, D., H., Entin, J.: NASA's SnowEx campaign: Observing seasonal snow in a forested environment, *2017 IEEE International Geoscience and Remote Sensing Symposium (IGARSS)*, DOI: 10.1109/IGARSS.2017.8127222, 2017.

King, M.D., Platnick, S., Menzel, W.P., Ackerman, S.A., Hubanks, P.A.: Spatial and temporal distribution of clouds observed by MODIS onboard the Terra and Aqua satellites, *IEEE Trans. Geosci. Remote Sens*. 51 (7), 3826–3852, 2013.

Klein, A.G. and Stroeve, J.: Development and validation of a snow albedo algorithm for the MODIS instrument, *Annals of Glaciology*, 34:45-52, 2002

Kokhanovsky, A. A. and Zege, E. P.: Scattering optics of snow, *Appl. Optics*, 43, 1589–1602, 2004

Kokhanovsky, A., Lamare, M., Di Mauro, B., Picard, G., Arnaud, L., Dumont, M., Tuzet, F., Brockmann, C., and Box, J. E.: On the reflectance spectroscopy of snow, *The Cryosphere*, 12, 2371–2382, https://doi.org/10.5194/tc-12-2371-2018, 2018.

Kokhanovsky, A., Lamare, M.; Danne, O., Brockmann, C., Dumont, M., Picard, G., Arnaud, L., Favier, V., Jourdain, B.; Le Meur, E., Di Mauro, B., Aoki, T., Niwano, M., Rozanov, V., Korkin, S., Kipfstuhl, S., Freitag, J., Hoerhold, M., Zuhr, A., Vladimirova, D., Faber, A.-K., Steen-Larsen, H.C., Wahl, S., Andersen, J.K., Vandecrux, B., van As, D., Mankoff, K.D., Kern, M., Zege, E., Box, J.E.: Retrieval of Snow Properties from the Sentinel-3 Ocean and Land Colour Instrument, *Remote Sens.*, 11, 2280, 2019.

Koren, I., Remer, L., Kaufman, Y. J., Rudich, Y., and Martins, J.: On the twilight zone between clouds and aerosols, *Geophys. Res. Lett.*, 34(8), L08805, doi:10.1029/2007GL029253, 2007.

LaChapelle, E. R.: Field Guide to Snow Crystals. University of Washington Press, 112 pp, 1969.

Lawson, P., Baker, B., Zmarzly, P., O'Connor, D., Mo, Q., Gayet, J.-F., and Shcherbakov, V.: Microphysical and optical properties of ice crystals at South Pole Station, *J. Appl. Meteor. Climatol.*, 45(11), 1505–1524, doi:10.1175/JAM2421.1, 2006.

Leroux C., and Fily M. : Modeling the effect of sastrugi on snow reflectance, *J. Geophys. Res.*, 103, 25,779-25,788, 1998.

Liu X. and Yanai M.: Influence of Eurasian spring snow cover on Asian summer rainfall, *International Journal of Climatology*, 22 (9), 1075-1089, https://doi.org/10.1002/joc.784,2002.

Liston, G. E., and C. A. Hiemstra: The Changing Cryosphere: Pan-Arctic Snow Trends (1979–2009). *J. Climate*, 24, 5691–5712, https://doi.org/10.1175/JCLI-D-11-00081.1, 2011

Libois, Q., Picard, G., Arnaud, L., Morin, S., and Brun, E.: Modeling the impact of snow drift on the decameter-scale variability of snow properties on the Antarctic Plateau, *J. Geophys. Res.*,119, 1662-11681,2014.

Lemke, P., J. Ren, R.B. Alley, I. Allison, J. Carrasco, G. Flato, Y. Fujii, G. Kaser, P. Mote, R.H. Thomas and T. Zhang: Observations: Changes in Snow, Ice and Frozen Ground. In: Climate Change 2007: The Physical Science

Basis. Contribution of Working Group I to the Fourth Assessment Report of the Intergovernmental Panel on Climate Change [Solomon, S., D. Qin, M. Manning, Z. Chen, M. Marquis, K.B. Averyt, M. Tignor and H.L. Miller (eds.)]. Cambridge University Press, Cambridge, United Kingdom and New York, NY, USA, 2007

Li, W., Stamnes, K., Chen, B., and Xiong, X.: Snow grain size retrieved from near-infrared radiances at multiple wavelengths, *Geophys. Res. Lett.*, 28, 1699–1702, doi:10.1029/2000GL011641, 2001.

Lyapustin, A. I.: Atmospheric and geometrical effects on land surface albedo. *Journal of Geophysical Research: Atmospheres*, 104(D4), 4127–4143. doi:10.1029/1998jd200064, 1999.

Lyapustin, A., Tedesco, M., Wang, Y.J., Aoki, T., Hori, M. and Kokhanovsky, A. : Retrieval of snow grain size over Greenland from MODIS, *Remote Sensing of Environment*, 113, 1976-1987,2009.

Lyapustin, A., Wang, Y., Xiong, X., Meister, G., Platnick, S., Levy, R., Franz, B., Korkin, S., Hilker, T., Tucker, J., Hall, F., Sellers, P., Wu, A., and Angal, A.: Scientific impact of MODIS C5 calibration degradation and C6+ improvements, *Atmos. Meas. Tech.*, 7, 4353-4365, https://doi.org/10.5194/amt-7-4353-2014, 2014.

Macke, A., Mueller, J., and Raschke, E.: Single scattering properties of atmospheric ice crystals, *J. Atmos. Sci.*, 53, 2813–2825, 1996.

Mary, A., Dumont, M., Dedieu, J.-P., Durand, Y., Sirguey, P., Milhem, H., Mestre, O., Negi, H. S., Kokhanovsky, A. A., Lafaysse, M., and Morin, S.: Intercomparison of retrieval algorithms for the specific surface area of snow from near-infrared satellite data in mountainous terrain, and comparison with the output of a semi-distributed snowpack model, *The Cryosphere*, 7, 741–761, https://doi.org/10.5194/tc-7-741-2013, 2013.

McFarlane, S. A., Marchand, R. T., and Ackerman, T. P.: Retrieval of cloud phase and crystal habit from Multiangle Imaging Spectroradiometer (MISR) and Moderate Resolution Imaging Spectroradiometer (MODIS) data, *J. Geophys. Res.-Atmos.*, 110, D14201, doi:10.1029/2004JD004831, 2005.

Mei, L. L., Rozanov, V., Vountas, M., Burrows, J., Levy, R., Lotz, W.: A Cloud masking algorithm for the XBAER aerosol retrieval using MERIS data. *Remote Sensing of Environment*. 197, 141-160, http://dx.doi.org/10.1016/j.rse.2016.11.016, 2017.

Mei, L.L., Rozanov, V., Vountas, M., Burrows, J.P.: The retrieval of ice cloud parameters from multi-spectral satellite observations of reflectance using a modified XBAER algorithm. *Remote Sensing of Environment*. 215(15),128-144,2018.

Mei, L., Vandenbussche, S., Rozanov, V., Proestakis, E., Amiridis, V., Callewaert, S., Vountas, M., Burrows, J. P., 2020, On the retrieval of aerosol optical depth over cryosphere using passive remote sensing, *Remote Sensing of Enviroment*, 241, 111731, https://doi.org/10.1016/j.rse.2020.111731, 2020a.

Mei, L.L., Rozanov, V., Ritter, C., Heinold, B., Jiao, Z.T., Vountas, M., Burrows, J.P.: Retrieval of aerosol optical thickness in the Arctic snow-covered regions using passive remote sensing: impact of aerosol typing and surface reflection model. *IEEE Transactions on Geoscience and Remote Sensing*. 10.1109/TGRS.2020.2972339, 1-15. 2020b.

Mei, L., Rozanov, V. and Burrows, J. P., : A fast and accurate radiative transfer model for aerosol remote sensing, *Journal of Quantitative Spectroscopy and Radiative Transfer*, 256,107270, 2020c

Mei, L., Rozanov, V., Pohl, C., Vountas, M. and Burrows, J. P.: The retrieval of snow properties from SLSTR/ Sentinel-3 - part 1: method description and sensitivity study, *The Cryosphere*, 2020d

Mei, L., Rozanov, V., A new snow bidirectional reflectance distribution function model in spectral regions from UV to SWIR in preparation, 2021

Montpetit, B., Royer, A., Langlois, A., Cliché, P., Roy, A., Champollion, N., Picard, G., Domine, F. and Obbard, R., Instruments and methods new shortwave infrared albedo measurements for snow specific surface area retrieval, Journal of Glaciolocy, 58 (211), 941 – 952, 2012.

Nakamura, T., O. Abe, T. Hasegawa, R. Tamura, and T. Ohta: Spectral reflectance of snow with a known particle-size distribution in successive metamorphism. *Cold Reg. Sci. Technol.*, 32, 13–26, https://doi.org/10.1016/S0165-232X(01) 00019-2, 2001.

Nakaya, U., Sekido, Y., General classification of snow crystals ad their frequency of occurrence. *J. Fac. Sci.*, Hokkaido Imperial Univ., Ser. II I-9, 234–264, 1938

Nakoudi, K.; Ritter, C.; Böckmann, C.; Kunkel, D.; Eppers, O.; Rozanov, V.; Mei, L.; Pefanis, V.; Jäkel, E.; Herber, A.; Maturilli, M.; Neuber, R. Does the Intra-Arctic Modification of Long-Range Transported Aerosol Affect the Local Radiative Budget? (A Case Study). *Remote Sens.*, 12, 2112, 2020.

Negi, H.S. and Kokhanovsky, A.: Retrieval of snow albedo and grain size using reflectance measurements in Himalayan basin, *The Cryospehre*, 5, 203-217,2011.

Painter, T. H., Dozier, J., Roberts, D. A., Davis, R. E., and Greene, R. O.: Retrieval of subpixel snow-covered area and grain size from imaging spectrometer data, *Remote Sens. Environ.*, 85, 64– 77, 2003.

Painter, T.H., Rittger, K., McKenzie, C., Slaughter, P., Davis, R.E., Dozier, J.: Retrieval of subpixel snow covered areas, grain size, and albedo from MODIS, *Remote Sensing of Environment*, 113, 868-879, 2009.

Picard, G., Libois, Q., Arnaud, L., Verin, G., and Dumont, M.: Development and calibration of an automatic spectral albedometer to estimate near -surface snow SSA time series, *The Cryosphere*, 10, 1297 – 1316, 2016.

Pirazzini, R., Räisänen, P., Vihma, T., Johansson, M., and Tastula, E.-M.: Measurements and modelling of snow particle size and shortwave infrared albedo over a melting Antarctic ice sheet, *The Cryosphere*, 9, 2357-2381, https://doi.org/10.5194/tc-9-2357-2015, 2015.

Platnick, S., Meyer, K.G., King, M.D., Wind, G., Amarasinghe, N., Marchant, B., Arnold, G.T., Zhang, Z.B., Hubanks, P., Holz, R., Yang, P., Lidgway, W. and Riedi, J.: The MODIS cloud optical and microphysical products: Collection 6 updates and examples from Terra and Aqua, IEEE Trans. Geosci. Remote Sens. 55 (1), 502 – 525, 2017.

Pohl C., Rozanov V.V. , Mei L. , Burrows J.P., Heygster G. and Spreen G.: Implementation of an ice crystal single-scattering property database in the radiative transfer model SCIATRAN, *J. Quant. Spectrosc. Radiat. Transfer*, doi: https://doi.org/10.1016/j.jqsrt.2020.107118,2020

Popp, T., de Leeuw, G., Bingen, C., Bruhl, C., Capelle, V., Chedin, A., Clarisse, L., Dubovik, O., Grainger, R., Griesfeller, J., Heckel, A., 5 Kinne, S., Kluser, L., Kosmale, M., Kolmonen, P., Lelli, L., Litvinov, P., Mei, L., North, P., Pinnock, S., Povey, A., Robert, C., Schulz, M., Sogacheva, L., Stebel, K., Stein Zweers, D., Thomas, G., Tilstra, L. G., Vandenbussche, S., Veefkind, P., Vountas, M., and Xue, Y.: Development, Production and Evaluation of Aerosol Climate Data Records from European Satellite Observations (Aerosol_cci), *Remote Sensing*, 8, 421, doi:10.3390/rs8050421, http://www.mdpi.com/2072-4292/8/5/421, 2016.

Räisänen, P., Makkonen, R., Kirkevåg, A., and Debernard, J. B.: Effects of snow grain shape on climate simulations: sensitivity tests with the Norwegian Earth System Model, *The Cryosphere*, 11, 2919-2942, https://doi.org/10.5194/tc-11-2919-2017, 2017.

Rittger, K., Painter, T. H. and Dozier, J.: Assessment of methods for mapping snow cover from MODIS, *Advances in Water Resources*, 51(35th Year Anniversary Issue), 367–380. doi:10.1016/j.advwatres.2012.03.002, 2013.

Rozanov, V. V., Rozanov, A. V., Kokhanovsky, A. A., and Burrows, J. P.: Radiative transfer through terrestrial atmosphere and ocean: Software package SCIATRAN, *J. Quant. Spect. Rad. Trans.* 133, 13–71, doi:10.5194/acp-8-1963-2008, 2014.

Rutter, N., J. Pan, M. Durand, J. King, C. Derksen, and F. Larue. : *SnowEx17 Laser Snow Microstructure Specific Surface Area Data, Version 1*. [Indicate subset used]. Boulder, Colorado USA. NASA National Snow and Ice Data Center Distributed Active Archive Center. doi: https://doi.org/10.5067/H9C1UVWN1UK3, 2018.

Ryan, J. C., Smith, L. C., van As, D., Cooley, S. W., Cooper, M. G., Pitcher, L. H., and Hubbard, A.: Greenland Ice Sheet surface melt amplified by snowline migration and bare ice exposure, *Science Advances*, 5, https://doi.org/10.1126/sciadv.aav3738, http://advances. sciencemag.org/content/5/3/eaav3738, 2019.

Saito, M., P. Yang, N. G. Loeb, and S. Kato: A novel parameterization of snow albedo based on a two-layer snow model with a mixture of grain habits, *J. Atmos. Sci.*, 76, 1419–1436, 2019.

Sarangi, C., Qian, Y., Rittger, K., Bormann, K. J., Liu, Y., Wang, H., Wan, H., Lin, G., and Painter, T. H.: Impact of light-absorbing particles on snow albedo darkening and associated radiative forcing over high-mountain Asia: high-resolution WRF-Chem modeling and new satellite observations, *Atmos. Chem. Phys.*, 19, 7105–7128, https://doi.org/10.5194/acp-19-7105-2019, 2019.

Sokratov, S. and Kazakov, N.: Dry snow metamorphism expressed by crystal shape, *Ann. Glaciol.*, 2012, vol. 58 (61), 51–56, 2012.

Stamnes, K., Li, W., Eide, H., Aoki, T., Hori,M. and Storvold, R.: ADEOSII/GLI snow/ice products - part I: Scientific basis, *Remote Sens. Environ.*, 111, 258–273, doi:10.1016/j.rse.2007.03.023, 2007.

Tanikawa T., Kuchiki K. , Aoki T. , Ishimoto H. , Hachikubo A. , Niwano M. , Hosaka M. , Matoba S. , Kodama Y. , Iwata Y. , and Stamnes K. : Effects of snow grain shape and mixing state of snow impurity on retrieval of snow physical parameters from ground - based optical instrument,*Journal of Geophysical Research: Atmospheres*, https://doi.org/10.1029/2019JD031858,2020

Tuzet, F., Dumont, M., Picard, G., Lamare, M., Voisin, D., Nabat, P., Lafaysse, M., Larue,F., Revuelto, J. And Arnaud L.: Quantification of the radiative impact of light-absorbing particles during two contrasted snow seasons at Col du Lautaret (2058 m a.s.l. French Alps), The Crosphere, 14, 4553 – 4579, 2020.

Thackeray, C. W. , & Fletcher, C. G. .: Snow albedo feedback Current knowledge, importance, outstanding issues and future directions. *Progress in Physical Geography*, 40(3), 392–408. doi:10.1177/0309133315620999, 2016.

Wiebe, H., Heygster, G., Zege, E., Aoki, T., and Hori, M.: Snow grain size retrieval SGSP from optical satellite data: Validation with ground measurements and detection of snow fall events, *Remote Sens. Environ.*, 128, 11–20, https://doi.org/10.1016/j.rse.2012.09.007, 2013.

Wendisch, M., Muller, D., Schell, D., and Heintzenberg, J.: An air- ¨ borne spectral albedometer with active horizontal stabilization, *J. Atmos. Oceanic Technol.*, 18, 1856–1866, 2001

Wendisch, M., Pilewskie, P., Jakel, E., Schmidt, S., Pommier, J., Howard, S., Jonsson, H. H., Guan, H., Schroder, M., and Mayer, B.: Airborne measurements of areal spectral surface albedo over different sea and land surfaces, *J. Geophys. Res.*, 109, D08203, doi:10.1029/2003JD004392, 2004.

Xiong, C., & Shi, J.: Snow specific surface area remote sensing retrieval using a microstructure based reflectance model. *Remote Sensing of Environment*, 204, 838–849. doi:10.1016/j.rse.2017.09.017,2018

Yamaguchi, S.; Hiroyuki, H.; Avanzi, F.: Daily summary of weather, snow, and preferential-flow conditions at the Snow and Ice Research Center, Nagaoka (Japan) - snow seasons 2006 through 2018. PANGAEA, https://doi.org/10.1594/PANGAEA.909880, 2019.

Yang, P., Bi, L., Baum, B. A., Liou, K.-N., Kattawar, G. W., Mishchenko, M. I. And Cole, B.: Spectrally consistent scattering, absorption, and polarization properties of atmospheric ice crystals at wavelengths from 0.2 to 100 µm, *J. Atmos. Sci.*.70, 330–347, 2013.

Zege, E. P., Kokhanovsky, A. A., Katsev, I. L., Polonsky, I. N., and Prikhach, A. S.: The retrieval of the effective radius of snow grains and control of snow pollution with GLI data. In M. I. Hovenier (Ed.), Proceedings of conference on light scattering by nonspherical particles: theory, measurements, and applications (pp. 288–290). Boston, Mass: *American Meteorological Society*, 1998.

Zege, E.P., Katsev, I.L., Malinka, A.V., Prikhach, A.S., Heygster, G. and Wiebe H.: Algorithm for retrieval of the effective snow grain size and pollution amount from satellite measurements, *Remote sensing of Environment*, 115, 2674-2685, 2011.

Zhang, T., Wang T., Krinner G., Wang, X., Gasser, T., Peng S., Piao S. and Yao T.: The weakening relationship between Eurasian spring snow cover and Indian summer monsoon rainfall. *Science advances*, 5(3), DOI: 10.1126/sciadv.aau8932, 2019.

Zhao, S., Jiang, T., Wang, Z.: Snow grain-size estimation using Hyperion imagery in a typical area of the Heihe river basin, China. *Remote Sens*., 5, 238–253, 2013.